BIOMATERIALS FOR THE CENTRAL NERVOUS SYSTEM

Contract No. NO1-NS-1-2338

Revised Final Report

March 8, 2006

The University of Michigan and
The University of Utah

David C. Martin and Patrick A. Tresco

Overview

This is an expanded final report on our recently completed NIH contract NO1-NS-1-2338, by Prof. David C. Martin of the University of Michigan and Prof. Patrick A. Tresco at the University of Utah. Here, we elaborate in more detail on what was accomplished during the course of the contract, what was not accomplished, and make suggestions for future research.

We first review the Specific Aims of the contract. We then list accomplishments, grouped according to each Specific Aim. We then outline the details of each accomplishment, including a descriptive paragraph, and specific references. Further details are available in Quarterly Progress Reports that were previously filed with the NIH on this Contract and in papers in the peer-reviewed press. We then list items that were not accomplished. Finally, we present several areas where we believe there are opportunities for future research.

Specific Aims of the Contract:

(1) Develop or select candidate matrix surfaces that are likely to enhance mechanical stability at the interface of a microelectrode array and neural tissue for a microelectrode implanted within the central nervous system.

(2) Select or develop candidate organic functional groups that are bound to or diffuse from the matrix surface and that are likely to enhance growth and/or adhesion of neurons or neuronal processes to specific regions of an implanted silicon microelectrode array.

(3) Develop or adapt methods to deposit a matrix with selected surface functional groups onto silicon microelectrode arrays. Microelectrode arrays shall be selected from the devices available at the Center for Neural Communication Technology (http://www.engin.umich.edu/center/cnct/) sponsored by the National Center for Research Resources.
(a) The matrix and functional groups shall be stable in saline at 37 C for at least three (3) months.
(b) The matrix shall remain adherent to the microelectrode following implantation through the pia-arachnoid into neural tissue.

(4) Select an in-situ animal model(s) of mammalian cortex (excluding chimpanzees) and investigate the growth and adhesion of neurons, glia, micro-glia, and other cells present in the nervous system on chronically implanted microelectrode arrays coated with the selected matrix. Studies shall be done with and without cables attached to the microelectrode arrays.

(5) Cooperate with other investigators in the Neural Prosthesis Program by coating microelectrodes (estimate 50 over the contract period) with the most promising materials for in-vivo evaluation. The microelectrodes will be supplied by the NINDS Project Officer.

What was achieved:

Specific Aim 1:
PEDOT can be electrochemically polymerized like polypyrrole
PEDOT copolymers using functionalized EDOT can be deposited electrochemically
PEDOT can be grown into well-defined porous structures
Fibrillar structures of PEDOT can be created
The mechanical properties of electrochemically deposited PEDOT coatings varies with thickness in a manner that correlates with their electrical properties and morphology
Finite-element studies confirm high strains near probe-tissue interface

Specific Aim 2:
Hydrogels can be deposited onto probes
Alginate coatings can be used to entrap living cells onto probe surfaces
Alginate coatings can be used to release anti-inflammatory agents such as naproxen and dexamethasone
PPy and PEDOT can be grown through hydrogel scaffolds
PEDOT networks grown on hydrogel scaffolds can be imaged by TEM
Nanotubes of PEDOT can be used for controlled drug release
Nanoparticles of PLGA can be used to incorporate drugs, controlled release
Collagen and NGF incorporated into PPy and PEDOT coatings are bioactive

Specific Aim 3:
PEDOT is more chemically stable than polypyrrole
Unmodified hydrogel coatings decrease acute probe recording quality
PEDOT can be grown inside nano-structured surfactant templates
Electrospun fibers can be oriented, used for directed cell regeneration
EDOT is not cytotoxic to cells for short periods of time and at low concentrations
EDOT can be grown around living cells in-vitro
EDOT can be grown around living cells in-vivo

Specific Aim 4:
Developed methods to examine the ability of candidate organic functional groups bound to microelectrode arrays to enhance the growth and/or adhesion of primary neural cells derived from rat cortex
The adherence of various CNS-derived cells can be influenced by microelectrode surface coatings
Cell attachment to electrode sites can be influenced by electronically conductive polymer coatings
Activated macrophages are attached to retrieved uncoated silicon microelectrode arrays and release neuroinflammatory and neurotoxic compounds
Developed an unbiased quantitative method to analyze the tissue response to implanted silicon microelectrode arrays
Implanted probes show a stratified cellular response consisting of microglia, activated glia, and neural loss around the probe

Tethering implanted microelectrodes to skull bone in the absence of electronic hardware elicits a similar tissue response to animals implanted with full electronic hardware headstage and cabling
Tethering increases cortical tissue reactivity to implanted silicon microelectrode arrays.
Tissue response to implanted silicon microelectrode array is unchanged at 12 weeks post implantation and does not vary with rat strain
Retrieved hydrogel coated microelectrode arrays contain hydrogel after 2, 4 and 12 weeks in rat cortex
Loss of neuron associated neurofilament is abrogated by hydrogel coatings
NGF incorporated into alginate coatings elicits a specific response in-vivo (ChAT)
Brain tissue reactivity is reduced adjacent to OEC-coated silicon microelectrode arrays
PEDOT coatings lead to improved recordings in-vivo

Specific Aim 5:
PEDOT can be coated on Utah multishank electrodes
PEDOT can be coated onto ball electrodes
PEDOT coated onto a wide variety of other electrodes (Stanford, Applied Biophysics, custom-designed geometries).
PEDOT coated onto cochlear implants, pacemakers

Aim 1: PEDOT can be electrochemically polymerized like polypyrrole

We examined the electrochemical polymerization of 3,4-ethylenedioxythiophene (EDOT) and found that like polypyrrole, it could also be readily deposited onto the surfaces of conducting electrodes by either galvanostatic or potentiostatic electrochemical deposition. The diethoxy side group donates charge to the conjugated polymer backbone, and prevents synthetic errors that lead to chemical instabilities (Figure 1).

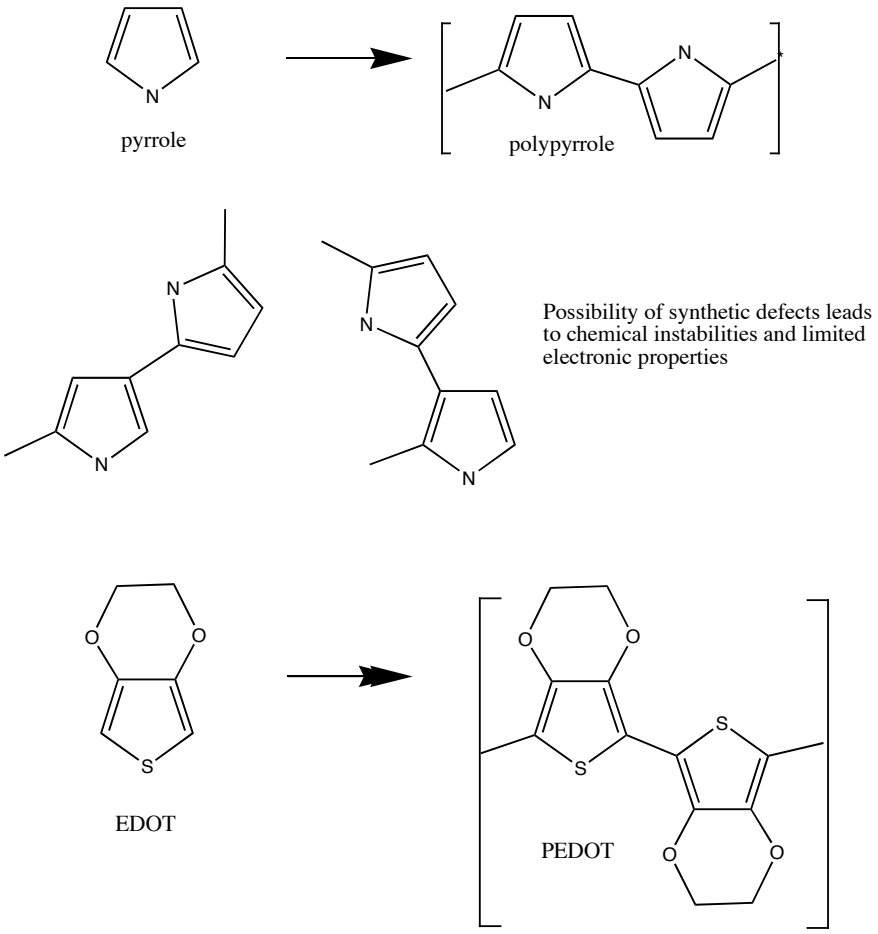

Chemical structures of polypyrrole and poly(3,4-ethylenedioxythiophene) (PEDOT). The extra hydrogens on the pyrrole monomer lead to the formation of chemical defects in polypyrrole that result in lower chemical stability of the chain. This is not possible in EDOT because there are only two hydrogens on the five-membered ring. Furthermore, the oxygens next to the conjugated ring system donates electronic charge, making the PEDOT molecule more electronically active.

References: Quarterly Report #1

Cui, X. & Martin, D. C. (2003). Electrochemical Deposition and Characterization of Poly(3,4-ethylenedioxythiophene) on Neural Microelectrode Arrays. *Sensors and Actuators B: Chemical*, *89*, 92-102.

Aim1: PEDOT copolymers using functionalized EDOT can be deposited electrochemically

We also found that derivatives of EDOT containing various hydrophilic side groups could be copolymerized with EDOT monomers onto neural probes.

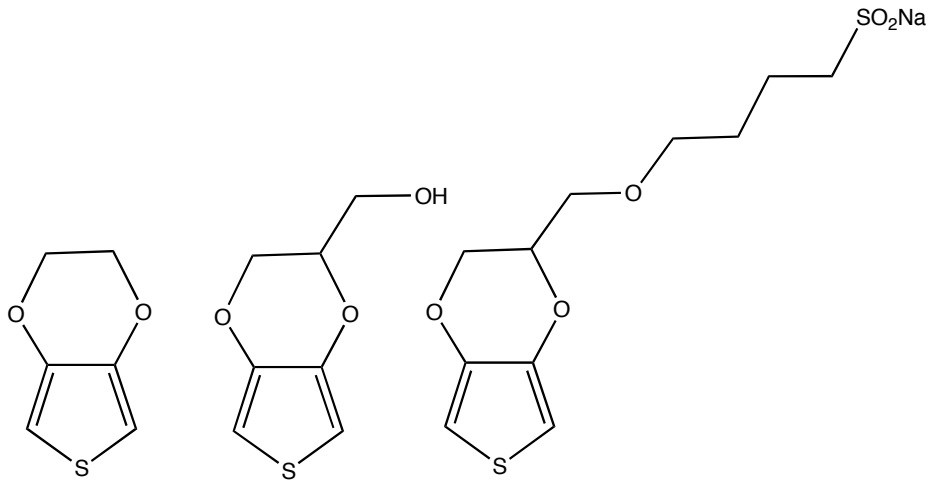

EDOT EDOT-MeOH S-EDOT

Chemical structures of functionalized variants of EDOT that could be electrochemically copolymerized with neat EDOT using procedures similar to those used to make EDOT homopolymer.

References: Quarterly Reports #1, #3

Xiao, Y., Cui, X., Hancock, J. M., Bogettaya, M., Reynolds, J. R., & Martin, D. C. (2004). Electrochemical Polymerization of Poly(hydroxymethylated-3,4-ethylenedioxythiophene) (PEDOT-MeOH) on Multichannel Neural Probes. *Sensors and Actuators B: Chemical*, *99*(2-3), 437-43.

Xiao, Y., Cui, X., & Martin, D. C. (2004). Electrochemical polymerization and properties of PEDOT/S-PEDOT on neural microelectrode arrays. *Journal of Electroanalytical Chemistry*, *573*, 43-48.

Aim 1: PEDOT can be grown into well-defined porous structures

We determined that polystyrene latex spheres could be used as templates to make PEDOT films with controlled variations in size of porosity. We found that best properties came from materials that had the smallest spheres that retained good order. These results indicate that for the best electrical properties, it is necessary to maintain a high degree of interconnections between holes (open-cell foam).

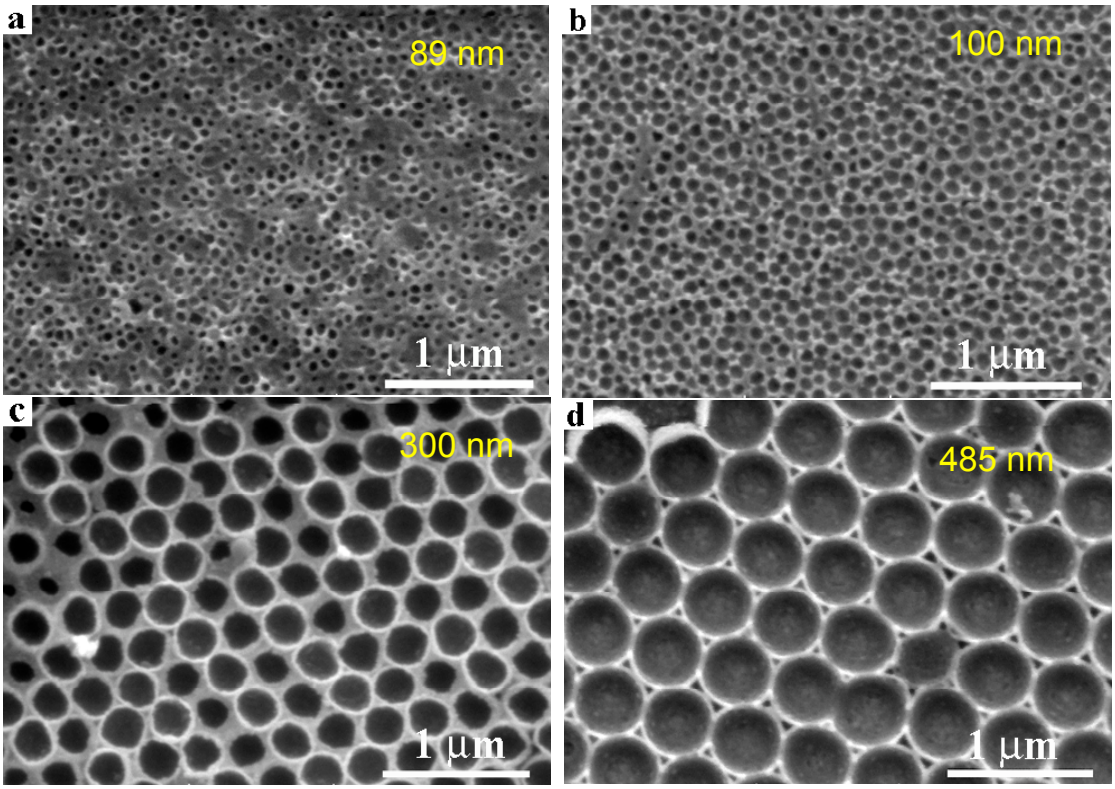

SEM images of PS-sphere templated PEDOT. The lowest impedance properties come from the spheres that have the smallest diameters yet still retain good order (here at 300 nm). This allows the film to have the highest amount of surface area with the pores remaining highly interconnected.

References: Quarterly Report #7

Yang, J. & Martin, D. C. (2004). Microporous Conducting Polymers on Neural Prosthetic Devices. II. Physical Characterization. *Sensors and Actuators A:Physical*, *113*(2), 204-11.

Yang, J. & Martin, D. C. (2004). Microporous Conducting Polymers on Neural Prosthetic Devices. I. Electrochemical Deposition. *Sensors and Actuators B: Chemical*, *101*(1-2), 133-42.

Aim 1: Fibrillar structures of PEDOT can be created

Certain synthetic polyanions can be incorporated into the reaction mixture, resulting in the reproducible formation of PEDOT nanofilaments. In particular, we found that poly(acrylic acid) solutions of an appropriate range of molecular weight (~550k) and concentration (~0.4 wt%) resulted in films with a consistent morphology of thin nanofilaments.

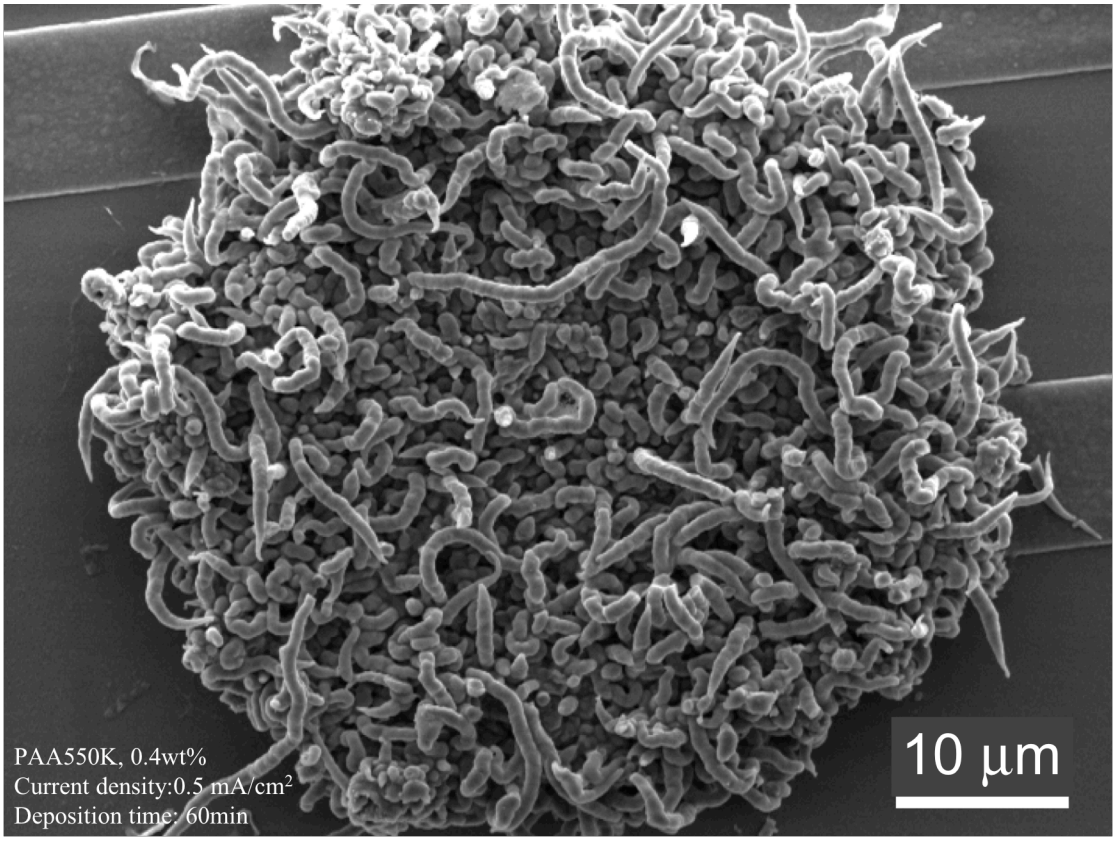

SEM image of a nanofibrous PEDOT film created using poly(acrylic acid) counterions with a molecular weight of 550,000 gms/mole at a concentration of 0.4 wt%, current density of 0.5 mA/cm2 and deposition time of 60 minutes.

References: Quarterly Reports #5, #10

Aim 1: The mechanical properties of electrochemically deposited conducting polymer coatings varies with thickness in a manner that correlates with their electrical properties and morphology

Nanoindentation of PEDOT coatings as a function of thickness showed that the effective modulus and hardness varied systematically in a manner that correlated with their electrical properties and surface morphology as measured by SEM and AFM. Specifically, as the films thicken they become fuzzier and softer, as well as more efficient at charge transport.

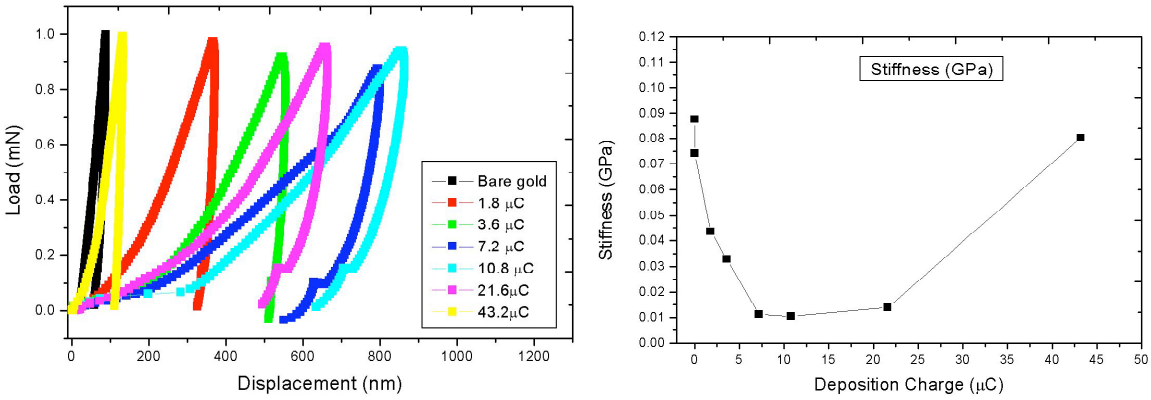

Left: Nanoindentation measurements of PEDOT films as a function of thickness / deposition charge. Right: Effective stiffness as a function of film thickness. The films first soften, and then become stiffer. This evolution in properties correlates with the evolution of transport properties measured by impedance spectroscopy, and is consistent with the development of a fuzzy surface morphology seen by microscopy.

Reference: Quarterly Reports #2, #12, #13

Yang, J. & Martin, D. C. (2006). Impedance Spectroscopy and Nanoindentation of Conducting PEDOT Coatings on Neural Prosthetic Devices. *Journal of Materials Research, in press.*

Aim 1: Finite-element studies confirm high strains near probe-tissue interface

Computer simulations of the mechanical stress and strain field around implanted probes revealed the high strains right near the tissue-electrode interface. The variation in strain as a function of distance from the probe surface was mapped, and compared with existing models for this distribution. The strains were smaller when softer substrates were used in the simulations. These results reveal the need to keep cells as far away from the probe surface as possible to avoid problems from these local strain gradients. It also demonstrates the benefits from using softer substrates.

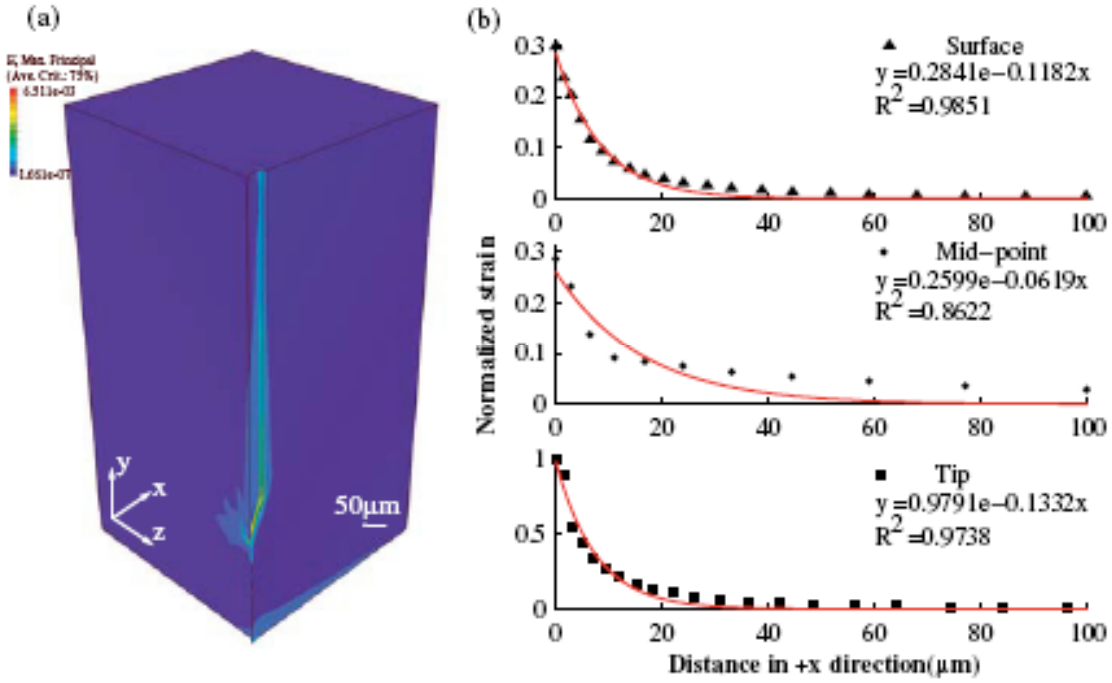

Left: distribution as a function of distance from the probe surface. Right: graphs of the strain distribution at various positions from the exterior (surface, mid-point, and tip). The highest strains are observed most proximal to the probe, with the most intense strains observed within the first 20-40 microns.

Reference: Subbaroyan, J., Martin, D. C., & Kipke, D. R. (2005). A finite-element model of the mechanical effects of implantable microelectrodes in the cerebral cortex. *Journal of Neural Engineering*, *2*, 103-13.

Aim 2: Hydrogels can be deposited onto probes

We developed a procedure for putting layers of hydrogels onto microfabricated neural probes using a sequential dipping technique.

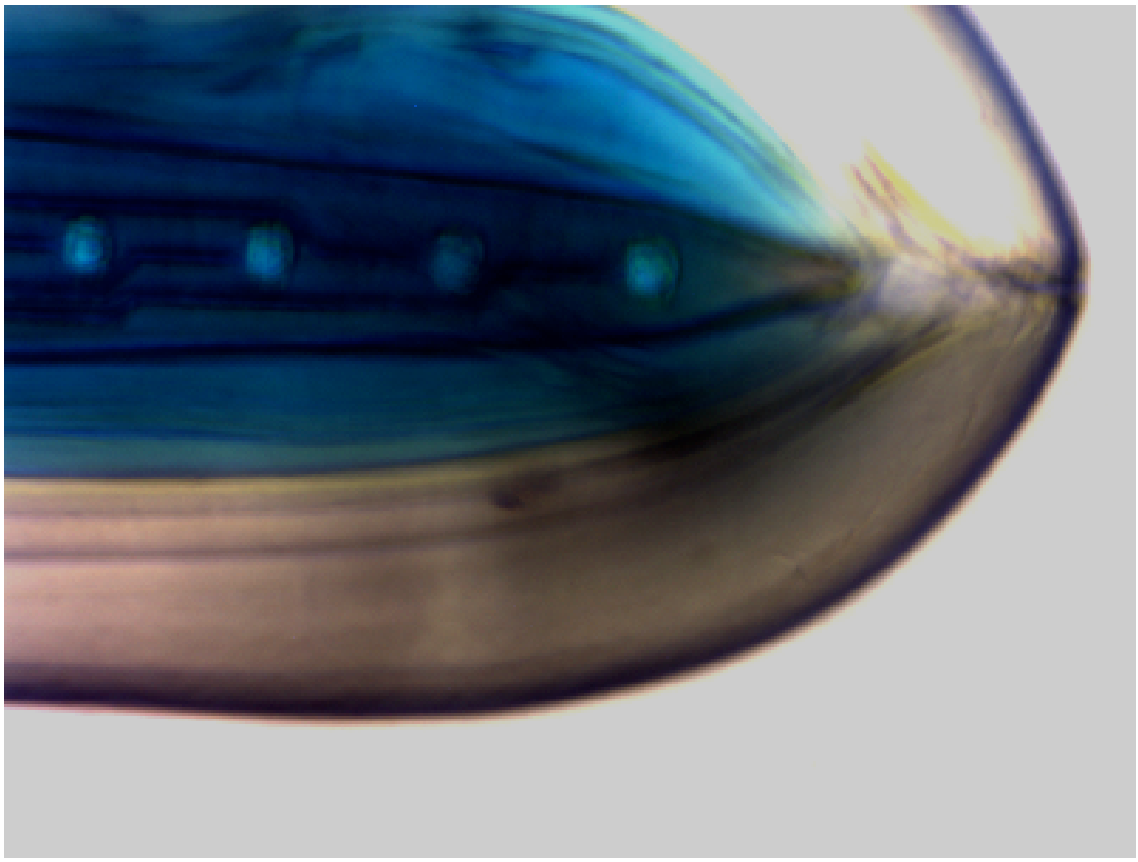

Optical micrograph of an alginate hydrogel-coated neural probe. The hydrogel was coated in eight layers, with the inner four layers containing dextran-blue and the outer four unmodified hydrogel.

References: Quarterly Report #1

Kim, D., Abidian, M., & Martin, D. C. (2004). Conducting Polymers Grown in Hydrogel Scaffolds Coated on Neural Prosthetic Devices. *Journal of Biomedical Materials Research*, *71A*(4), 577-85.

Kim, D. (2005). *Surface Modification of Neural Prosthetic Devices by Functional Polymers Incorporating Neurotrophic & Pharmacological Agents,* Ph.D Dissertation, The University of Michigan, Ann Arbor, MI.

Aim 2: Alginate coatings can be used to entrap living cells onto probe surfaces

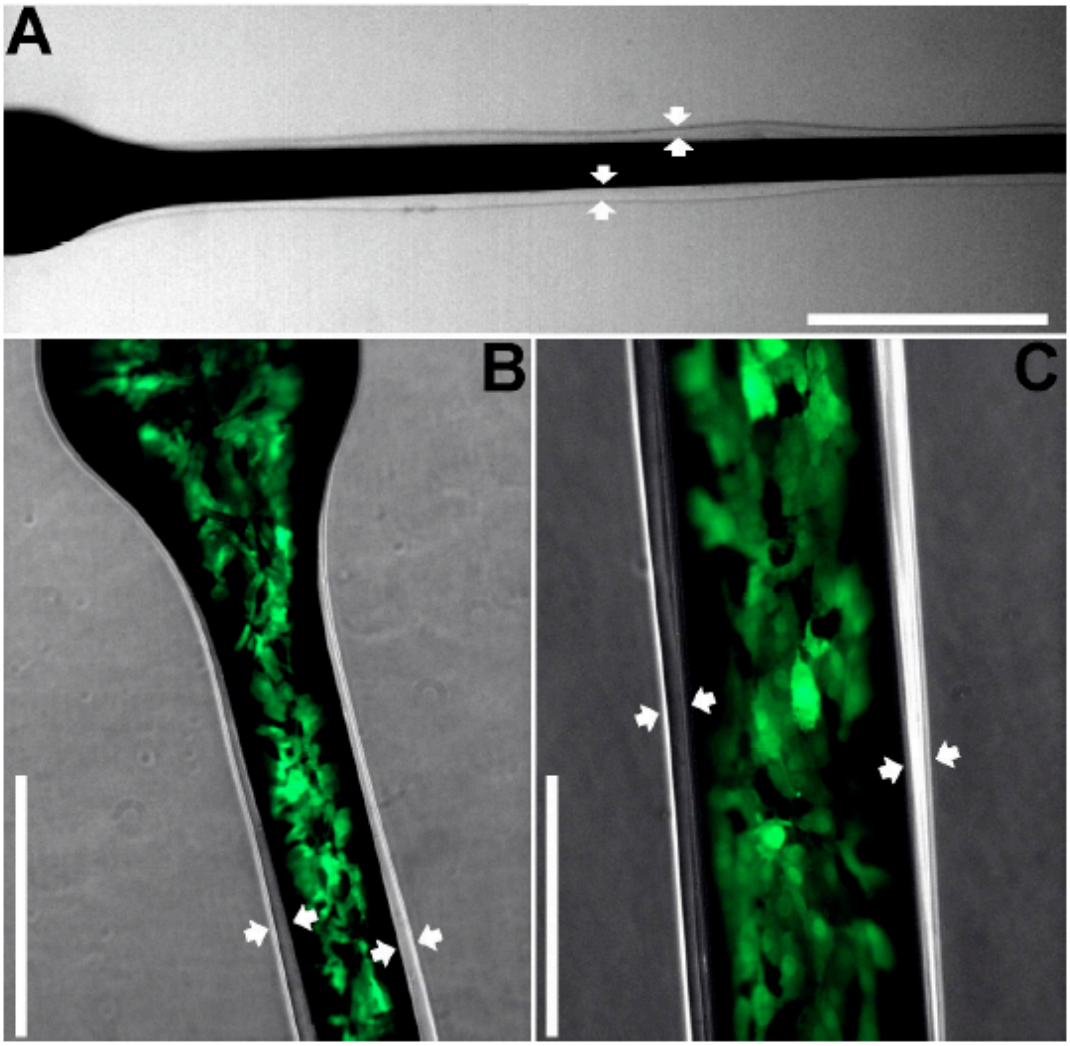

Figure U11-6. Alginate coated microelectrodes for entrapping cellular coatings. GFP-labeled adult olfactory ensheathing cells (OEC) isolated from Fischer 344 rat olfactory bulbs were cultured on the surfaces of microelectrodes. After reaching confluence, the cell-coated electrodes were encapsulated in a thin conformal coating of an alginate hydrogel seen as a clear thin film indicated in the above panels with the white arrows. Coating thickness surrounding the electrodes shown above averaged 30 microns. Scale bars = 1 mm (A), 500 µm (B), 250 µm (C).

Reference: Quarterly Report #11

Aim 2: Alginate coatings can be used to release anti-inflammatory agents such as naproxen and dexamethasone

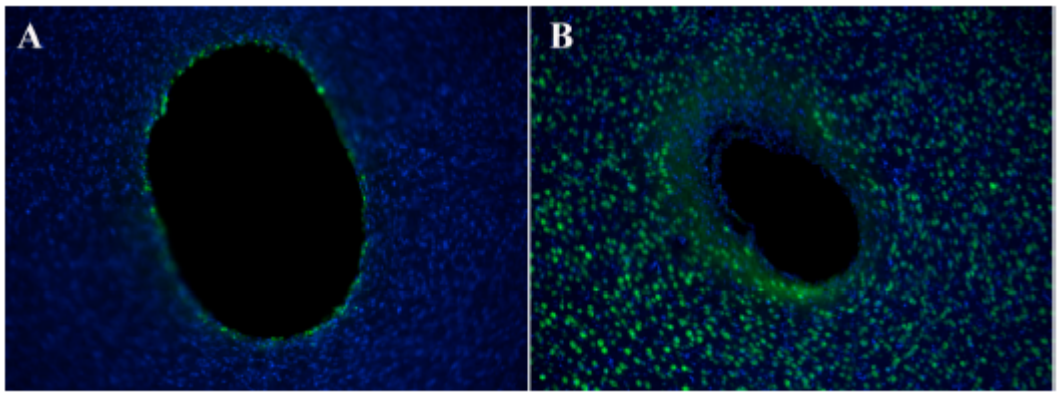

Figure U11-7. Cortical brain tissue response to microelectrodes coated with alginate releasing the anti-inflammatory agent Naproxen. Representative 20X image of horizontal sections at the level just above the recording sites stained for ED-1 (left panel A) showing a thin, single layer of ED-1+ cells (green) at the alginate brain tissue interface, and, in the same animal near the tip of the microelectrode array adjacent to the recording sites where the electrode tapers showing a reduction of NeuN immunoreactivity (green). In both panels above cell nuclei stained with DAPI appear blue. Similar results where observed with the water soluble and water insoluble dexamethasone alginate coatings.

Reference: Quarterly Report #11

Aim 2: PPy and PEDOT can be grown through hydrogel scaffolds

We demonstrated that both polypyrrole (PPy) and PEDOT could be grown through the hydrogel as a scaffold, resulting in a low density, low impedance, soft coating on the electrode.

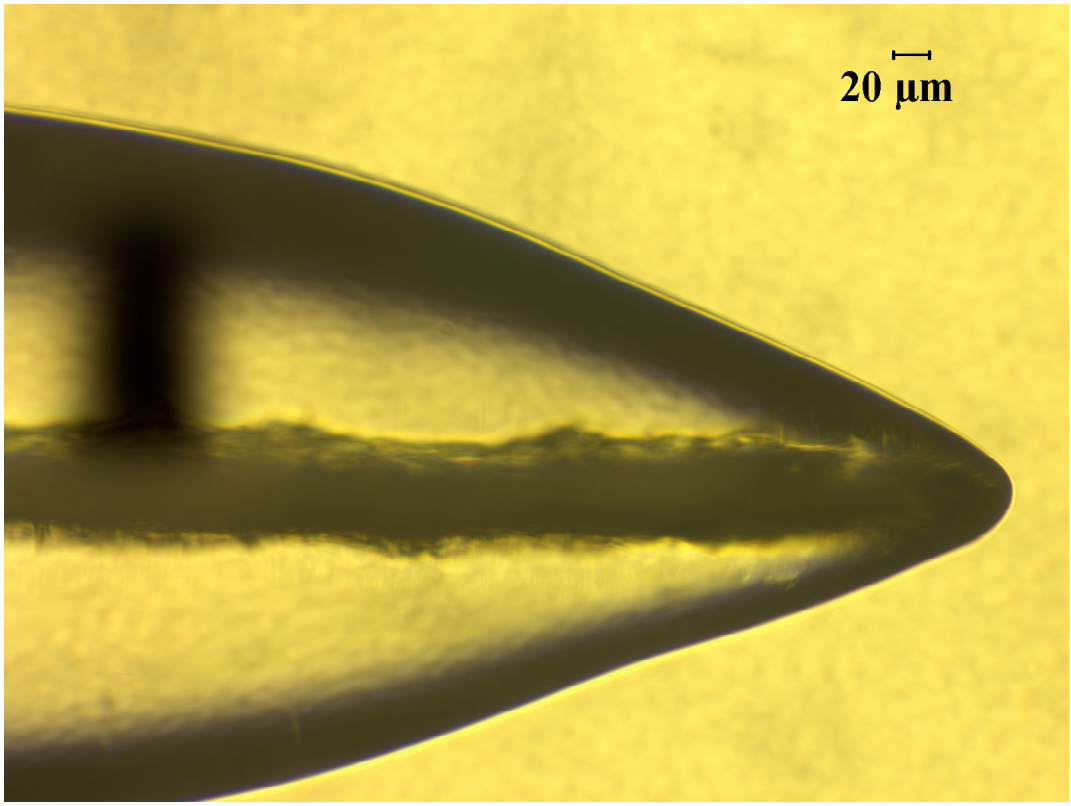

Side-view of hydrogel coated probe, with PEDOT electrochemically polymerized off an individual electrode up and through the hydrogel to the outer surface. A thin layer of electrospun nanofibers of PLGA are present on the probe surface.

References: Quarterly Reports #3, #4, and #5

Kim, D., Abidian, M., & Martin, D. C. (2004). Conducting Polymers Grown in Hydrogel Scaffolds Coated on Neural Prosthetic Devices. *Journal of Biomedical Materials Research*, *71A*(4), 577-85.

Aim 2: PEDOT networks grown on hydrogel scaffolds can be imaged by TEM

We developed a procedure for imaging the conducting-polymer infiltrated hydrogel scaffolds using transmission electron microscopy (TEM). These methods were adapted from procedures used to image tissues by TEM, and were developed in consultation with Dotty Sorenson of the Microscopy and Imaging Laboratory (MIL) at the University of Michigan Medical School. The images allowed us to visualize the hydrogel network both before and after PEDOT electropolymerization.

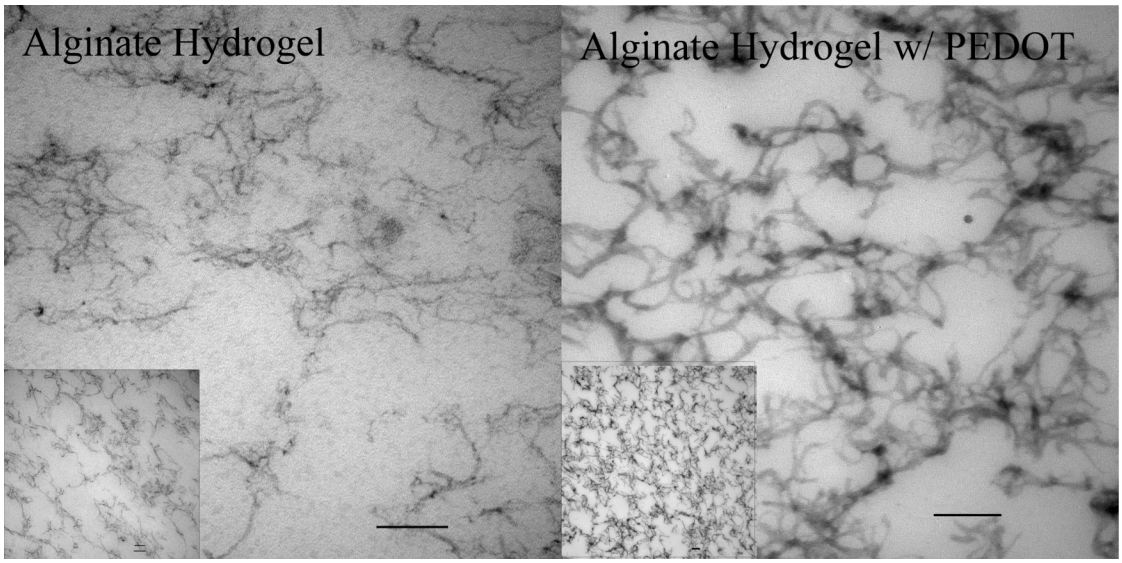

Left: TEM image of unmodified alginate hydrogel. Right: alginate hydrogel coated with PEDOT. The PEDOT causes an increase in the diameter of the filaments, but the open nature of the network remains intact. Scale bars = 100 nm.

Referemces: Quarterly Report #16

Aim 2: Nanotubes of PEDOT can be used for controlled drug release

We determined the nanofibers of biodegradable polymers such as PLGA could be loaded with drugs such as dexamethasone and deposited onto the surface of a neural probe. We then found that PEDOT could be grown around the nanofibers to create nanotubes. Finally, we demonstrated that these nanotubes could be stimulated externally to release controlled amounts of dexamethaszone from the probe surface at desired points in time.

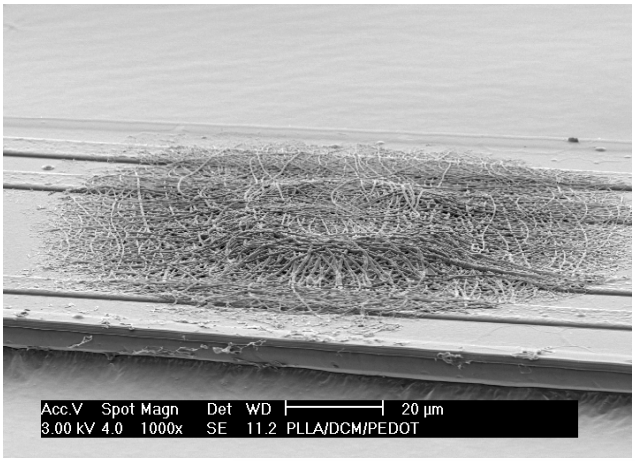

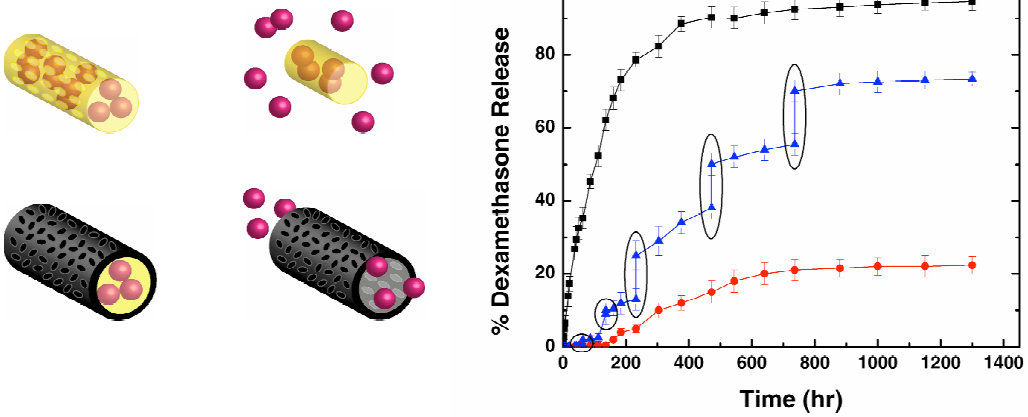

Top: SEM image of PEDOT nanotubes deposited on the surface of a neural probe. Lower left: schematic of drug release due to the external electrical stimulation of the PEDOT nanotubes. Lower right: controlled release of dexamethasone (DEX) from the PEDOT nanotubes. The unmodified tubes show relatively rapid release of the DEX, whereas the PEDOT-coated tubes show slow release. External stimulation allows for controlled released of the DEX at specfied points in time, (circled).

References: Quarterly Reports #7, #10, #12, and #15

Abidian, M. & Martin, D. C. (2005). Conducting Polymer Nanotubes for Controlled Drug Release. *Advanced Materials*, *18*, 405-09.

Aim 2: Nanoparticles of PLGA can be used to incorporate drugs, controlled release

We determined that dexamethasone could be incorporated into ~500 nm nanoparticles, and these nanoparticles could be incorporated into hydrogels on the surface of neural probes. The nanoparticle-functionalized probes show controlled release of the DEX, and probes modified with these coatings maintained low impedance when implanted acutely into Guinea Pig cortex.

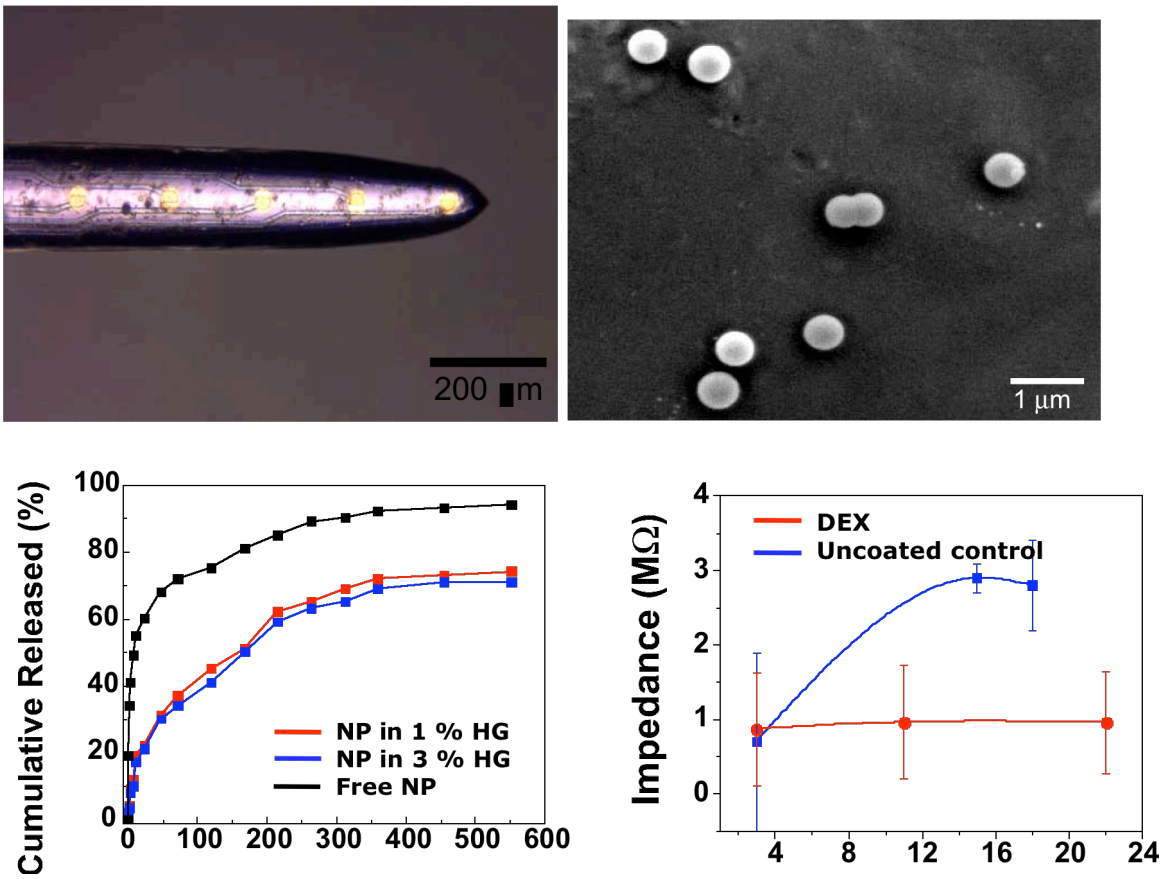

Upper left: hydrogel-coated neural probe containing DEX-loaded nanoparticles of PLGA. Upper right: SEM image of DEX-loaded nanoparticles. Lower left: controlled release of DEX from nanoparticles, as compared with free nanoparticles. The release occurs over a two-week period, consistent with the biological healing response seen in-vivo. Lower right: the impedance of the coatings containing DEX remains low, whereas the uncoated controls increase significantly.

References: Quarterly Reports #3, #10, #11, and #14

Kim, D.-H. & Martin, D. C. (2006). Sustained release of dexamethasone from hydrophilic matrices using PLGA nanoparticles for neural drug delivery. *Biomaterials*, *27*(15), 3031-37.

Aim 2: Collagen and NGF incorporated into PPy and PEDOT coatings are bioactive

Studies of the bioactivity of NGF modified PPy and PEDOT confirmed that these materials were able to induce neurite outgrowth in PC12 cells in-vitro. Collagen modified controls showed cell adhesion but no neurite extension, where as unmodified PEDOT showed little or no cell adhesion. These results confirm that both collagen and NGF proteins retain their bioactive nature even after electrochemical polymerization.

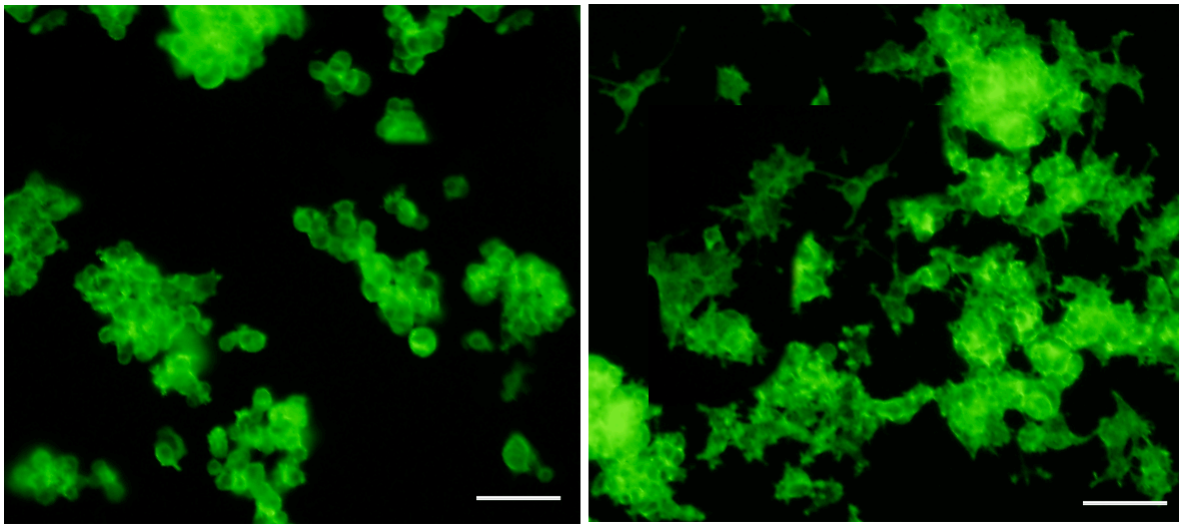

Left: Collagen-PEDOT. The cells adhere but do not send out processes. Right: NGF-PEDOT. The cells are adherent and also develop neurites. Unmodified PEDOT controls show little or no cell adhesion. Scale bars: 25 microns.

References: Quarterly Reports #3, #6, and #8

Kim, D.-H., Richardson-Burns, S. M., Hendricks, J., Sequera, C., & Martin, D. C. (2006). Effect of Immobilized Nerve Growth Factor (NGF) on Conductive Polymers: Electrical Properties and Cellular Response. *Advanced Functional Materials*, *in press*.

Aim 3: PEDOT is more chemically stable than polypyrrole

CV and impedance spectroscopy of both PEDOT and PPy showed that PEDOT was much more chemically stable than PPy (Figure 2). We therefore focused considerable additional attention on studies of EDOT since it was both more stable and more electronically active.

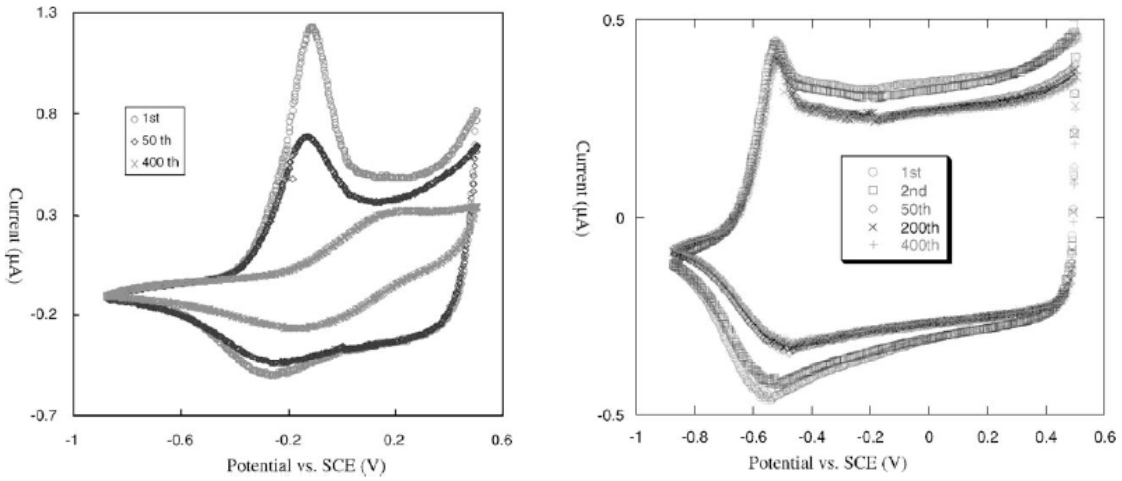

Cyclic voltammetry of polypyrrole (left) and PEDOT (right) as a function of cycle number at a scan rate of 0.1 V/sec. The area enclosed inside the cycle is a measure of charge capacity. The electrical properties of the PEDOT are much more stable than PPy, as indicated by the large charge capacity with extended cycling.

References: Quarterly Report #1

Cui, X. & Martin, D. C. (2003). Electrochemical Deposition and Characterization of Poly(3,4-ethylenedioxythiophene) on Neural Microelectrode Arrays. *Sensors and Actuators B: Chemical*, *89*, 92-102.

Aim 3: Electrospun fibers can be oriented, used for directed cell regeneration

We found that electrospun fibers could be oriented by spinning onto a rapidly rotating wheel, and that neural cells culture on the fibers would regenerate in a directed fashion. The oriented nanofibrous scaffolds caused the cells to align and grow in a preferred direction.

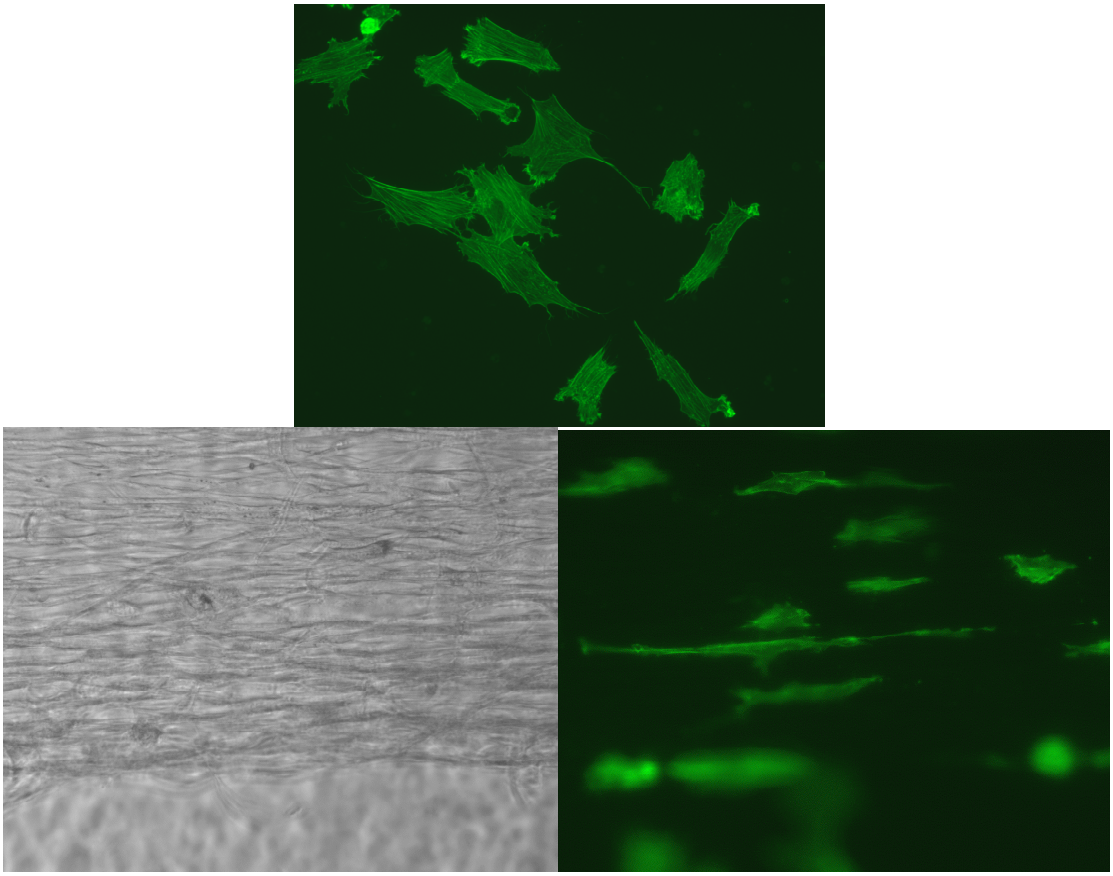

S-type human neuroblastoma cells (SY5Y), fixed in formaldehyde, stained with phalloidin (actin), conjugated to Oregon Green. Top: grown on a glass substrate. The cells are randomly oriented on the surface and equiaxed in shape. Lower left: fluorescent optical micrograph of oriented nanofibers (orientation direction left to right). Lower right: corresponding fluorescent micrograph showing the SY5Y cells elongated parallel to the nanofiber orientation direction. The high degree of induced alignment was also seen in dorsal root ganglia (DRG) cultures.

Reference: J. Corey, D. Y. Lin. S. Samuel, E. L. Feldman, and D. C. Martin, Nature Biotechnology, in review

Aim 3: Unmodified hydrogel coatings decrease acute probe recording quality

We found that unmodified hydrogel coatings alone would reduce recording quality in acute experiments. This is presumably due to a proximity effect, with the thicker coatings moving the targeted neurons farther away from the recording electrode surface.

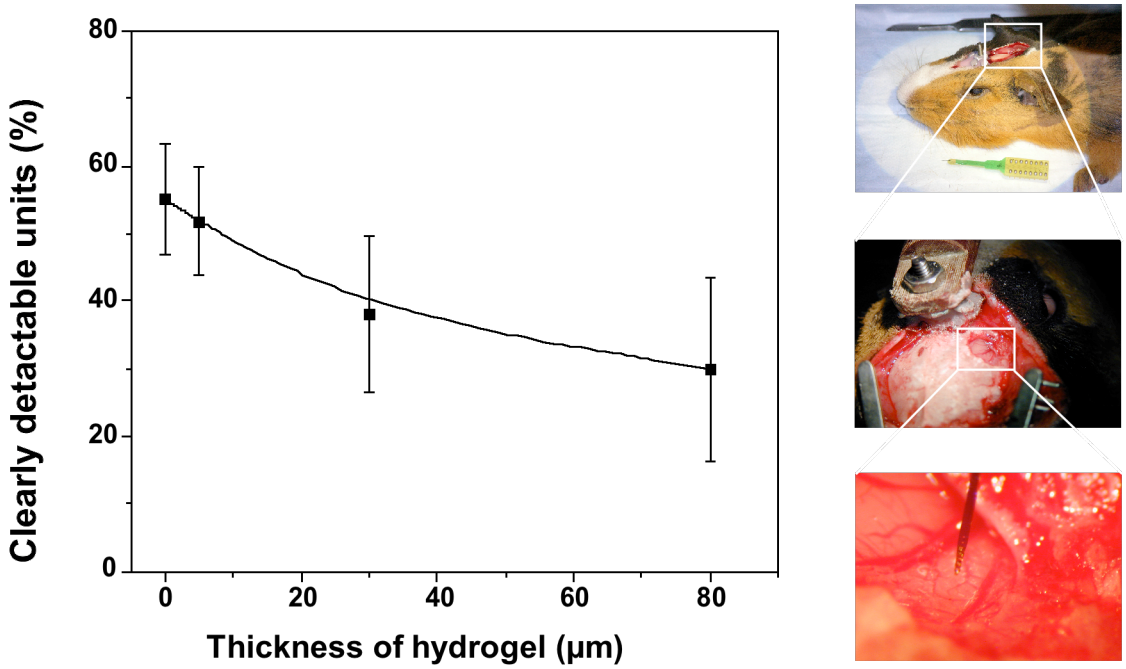

Left: Number of clearly detectable units as a function of the thickness of the alginate hydrogel coating. Right: details of the acute surgery on guinea pigs. Done in collaboration with James Wiler and David Anderson in the Kresge Hearing Research Institute.

References: Quarterly Reports #11, #13

Aim 3: PEDOT can be grown inside nano-structured surfactant templates

Certain non-ionic surfactants can be used to create a templated structure with extremely small pore sizes. This was demonstrated on hexagonally ordered filaments.

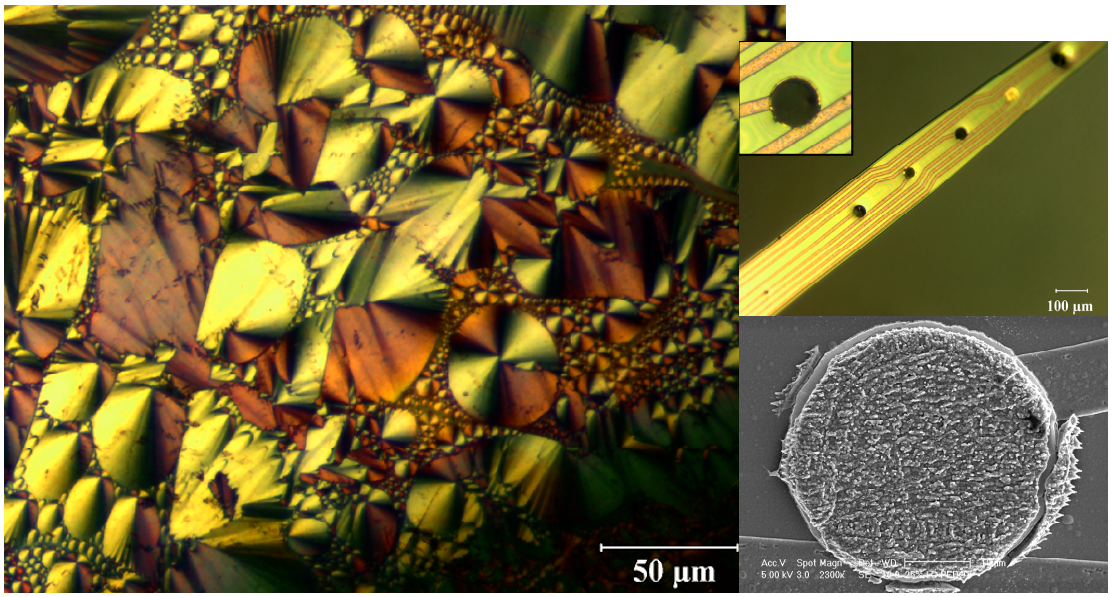

Left: optical micrograph of a PEDOT film grown within an ordered surfactant template. Upper right: optical micrograph of surfactant-templated PEDOT deposited directly on neural electrodes. Lower right: SEM image of a surfactant-templated PEDOT film deposited on a neural probe electrode.

References: Quarterly Report #11

Yang, J., Kim, D., Hendricks, J., & Martin, D. C. (2005). Ordered Surfactant-Templated Poly(3,4-ethylenedioxythiophene) (PEDOT) Conducting Polymer on Microfabricated Neural Probes. *Acta Biomaterialia*, *1*(1), 124-36.

Aim 3: EDOT is not cytotoxic to cells for short periods of time and at low concentrations

We examined the biological response of neurons to EDOT monomer and PSS counterion at various concentrations, and measured cell death after periods of 24 and 48 hours. We found that the EDOT monomer solution was not cytotoxic if the exposure times were limited an the concentration was kept below 0.01M. This corresponds to the concentration needed to conduct the electrochemical polymerization of EDOT.

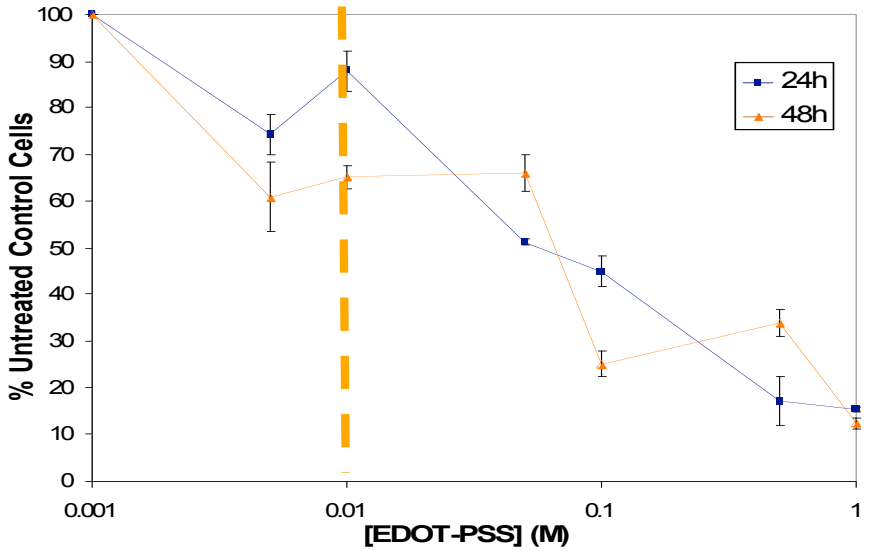

Graph of the cytotoxicity of EDOT monomer – PSS counterion solution at 24 hours and 48 hours as a function of solution concentration. The cells remain viable for limited exposure times and low concentrations.

References: Quarterly Report #12

Aim 3: EDOT can be grown around living cells in-vitro

We found that PEDOT could be electrochemically grown up and around living cells in-vitro. The PEDOT grew off the electrode around the cells, but did not grow directly underneath the cells where they were in close contact with the substrate. After sufficiently long polymerization times the cells could be completely encapsulated in PEDOT.

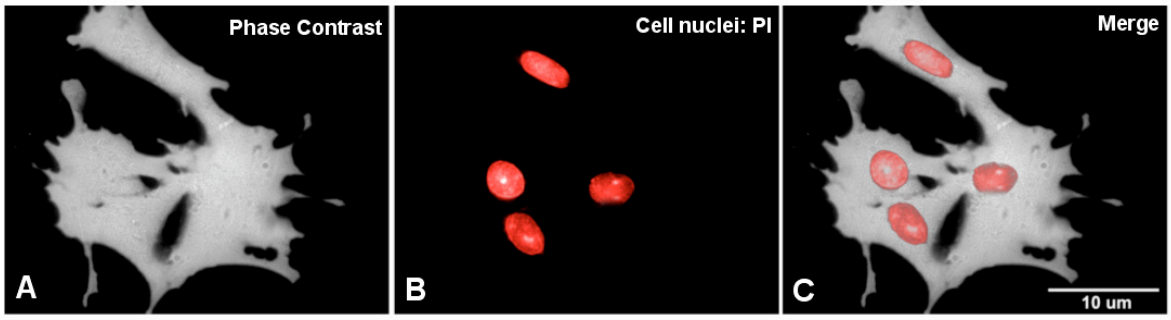

A: Phase contrast image of cells around which PEDOT has been electrochemically deposited. The dark background is the opaque, electrochemically deposited PEDOT. Note that the PEDOT film does not grow under the cells themselves. B: Cell nuclei stained with propidium iodide. C: Merged image.

References: Quarterly Reports #12 and #15

Aim 3: EDOT can be grown into PEDOT around living cells in-vivo

We determined that slices of brain could be exposed to EDOT monomer and the PEDOT polymer electrochemically polymerized within the living tissue. The images show PEDOT polymerized for various periods of time through the living CNS tissue. The higher magnification view shows that the PEDOT grew out and into the brain for distances of order 500 microns from the inserted microwire electrode. This is well beyond the typical size of the reactive glial inflammation and loss of neurons typically seen near an inserted probe (~150 microns). The example shown here is for brain, but we have also confirmed that this approach works in muscle and skin.

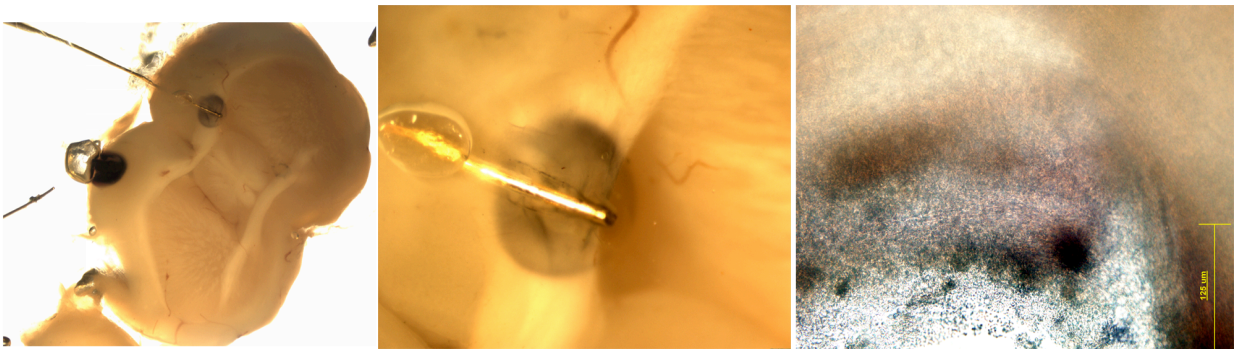

Left: low magnification view of brain slice where PEDOT has been polymerized for 15, 30, and 45 minutes at various locations. Middle: higher magnifcation view of the 30 minute polymerization showing a dark cloud of PEDOT that has grown off the microwire surface for about 500 microns into the surround tissue. Right: higher magnification shows a diffuse PEDOT network that has developed, presumably by growing through the extracellular space around the electrode surface.

References: S. Richardson-Burns et al., paper under external review at Science.

Aim 4: Developed methods to examine the ability of candidate organic functional groups bound to microelectrode arrays to enhance the growth and/or adhesion of primary neural cells derived from rat cortex

The results indicated that it was possible to develop genetically engineered cell coatings for the delivery of biologically active agents to the adjacent CNS tissue.

Figure U1-2

U1-2: Astrocyte and meningeal fibroblasts cultured on acute microelectrodes in vitro. The left panel of each set is the brightfield image of the same field. Astrocytes were immunostained for GFAP (green) and counterstained with DAPI (blue). Meningeal fibroblasts were immunostained for vimentin (red) and DAPI. Scale bars = 0.5mm.

Reference: Progress report #1

Aim 4: The adherence of various CNS-derived cells can be influenced by microelectrode surface coatings

Silicon microelectrode arrays were coated with electrospun silk-like polymers containing laminin moieties (SLPL) compared with uncoated electrodes and conventional glass surfaces. The number of adherent cells per electrode or per viewing field (for the glass control) was quantified after 24 hours of static culture conditions in 10% serum containing medium. All cell numbers are reported normalized to surface area (mean +/- standard error of the mean). Each condition is represented with at least n=6. For the purpose of comparison between cell populations, the final graph (bottom right) plots attached cells as a fraction of their corresponding glass control values. * indicates significance in student's t-test at $p<0.05$. Complete figures and description in Progress report 3.

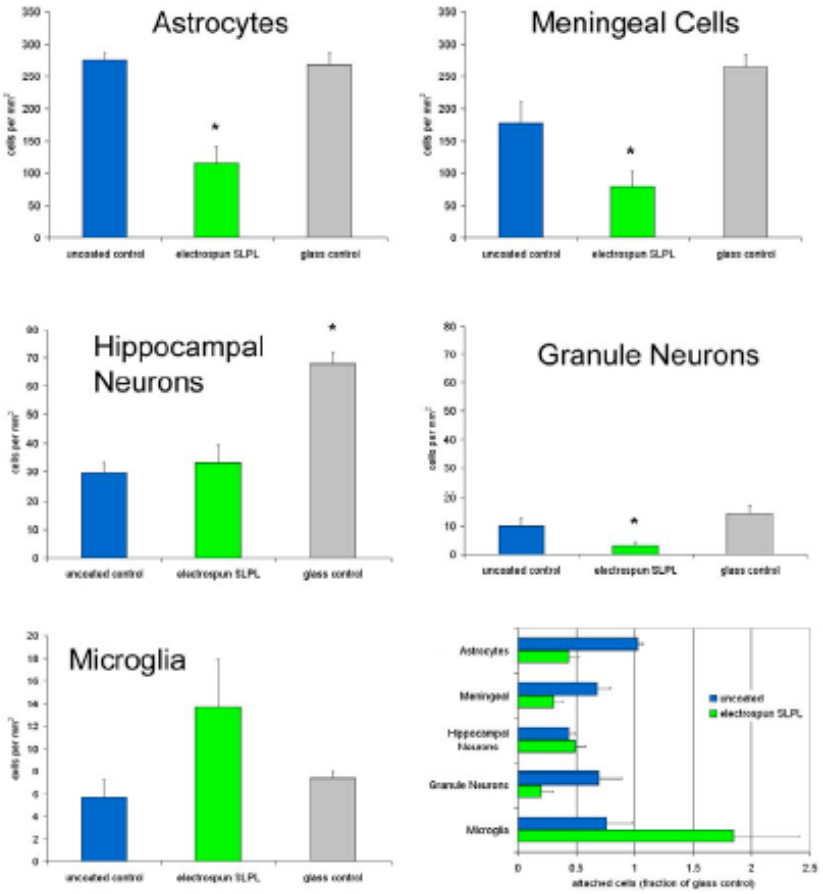

Reference: Quarterly Report #3.

Aim 4: Cell attachment to electrode sites can be influenced by electronically conductive polymer coatings

The results below show representative data from a study of the comparison of cell attachment between uncoated electrodes (iridium sites) and electrode containing sites treated with a polypyrrole-CDPYIGSR peptide blend. Cell attachment was normalized to unit surface area and reported as mean +/-standard error of the mean. * indicates significance by a student's t-test with $p<0.05$.

Table U3-1
In Vitro Cell Attachment to Electrode Sites

	Uncoated				CDPYIGSR			
cell type	total sites	average # in contact	expected	observed / expected	total sites	average # in contact	expected	observed / expected
astrocytes	144	5.2 +/- 0.61	0.93	5.6	24	10.0 +/- 1.88	1.10	9.1
meningeal fibroblasts	96	2.5 +/- 1.16	0.60	4.2	12	11.0 +/- 4.30	0.86	12.8
hippocampal neurons	192	0.2 +/- 0.12	0.10	2.0	20	0.6 +/- 0.27	0.14	4.3
granule neurons	192	0 +/- 0	0.03	0.0	24	0 +/- 0	0.03	0.0
microglia	192	0.1 +/- 0.02	0.02	5.0	24	0 +/- 0	0.08	0.0

* expected cells attached based on the surface area fraction of the sites to the bulk electrode

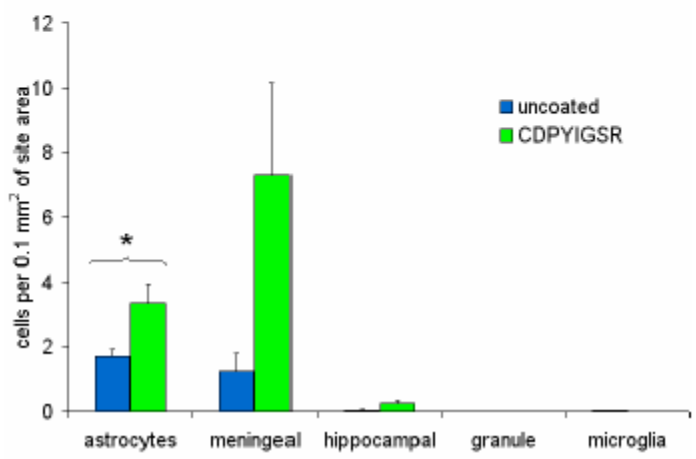

Reference: Quarterly Report #3

Aim 4: Activated macrophages are attached to retrieved uncoated silicon microelectrode arrays and release neuroinflammatory and neurotoxic compounds

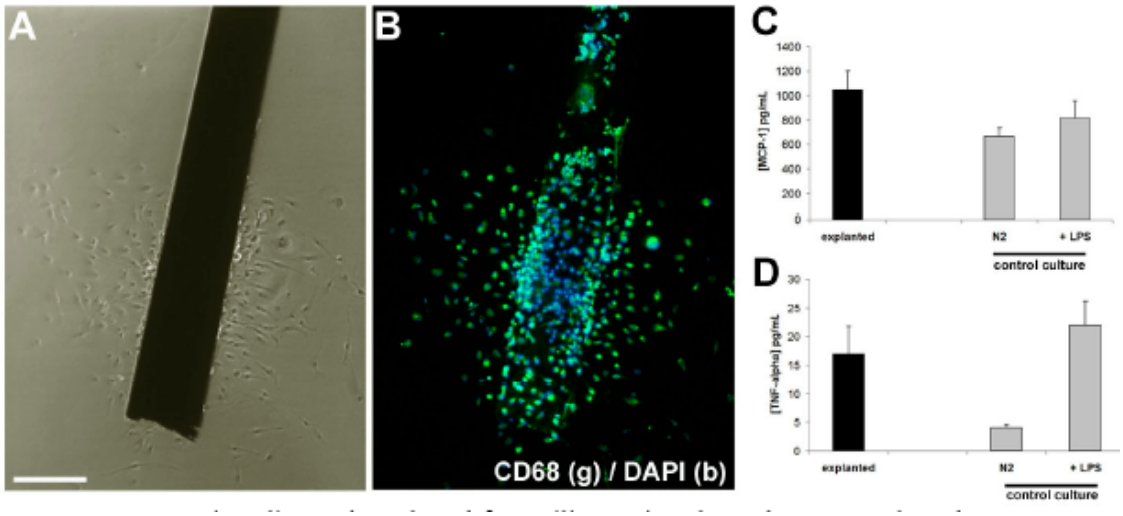

Figure U11-2. Microglia can be cultured from silicon microelectrode array explanted from rat motor cortex and produce pro-inflammatory cytokines. A,B) Representative phase contrast and corresponding fluorescence image of a fixed explanted electrode showing evidence of predominantly microglia. The electrode was implanted for 1 week, retrieved and cultured for 1 week. Scale bar = 200 microns. Serum-free medium condition from the first 24 hours of culture contained levels of MCP-1 and TNF_ comparable to LPS (1 µg/mL for 24 hours)-stimulated microglia harvested from postnatal Fischer 344 pups in conventional control cultures. N2 indicates the basal serum-free medium condition, which is DMEM/F12 supplemented with N2 components compared to LPS stimulated release. Of note is the fact that the post-natal derived microglia cultures contained approximately 10X the number of cells in the explant culture.

Reference: Quarterly Reports #11 and #12.

Biran, R., Martin, D. C., & Tresco, P. A. (2005). Neuronal cell loss accompanies the brain tissue response to chronically implanted silicon microelectrode arrays. *Experimental Neurology*, *195*(1), 115-26.

Aim 4: Developed an unbiased quantitative method to analyze the tissue response to implanted silicon microelectrode arrays

The fluorescence intensity of any stained section can be quantified and expressed as mean pixel intensity as function of distance from the implant interface. Using this approach it is possible to compare the response as a function of any given variable using standard and objective criteria that can be compared with statistical methods. Serial brain sections are first collected. For any desired immunostain, a series of evenly spaced sections along the implant interface are batch stained using the same solutions and conditions, and then mounted. Images of immunostained sections are viewed and captured by a PMT device mounted on a laser scanning confocal microscope. Images are stored as unsaturated 8 bit TIF files. For any given session where many images are captured, the same acquisition settings are used (PMT voltage, scan time, capture resolution, laser intensity, etc.). The settings are determined so that all images are of sufficient brightness for viewing, but the vast majority of pixels are not saturated. Single optical sections are collected and stored for each sample. The method although time consuming allows a direct statistical comparison of electrode coating on brain tissue response.

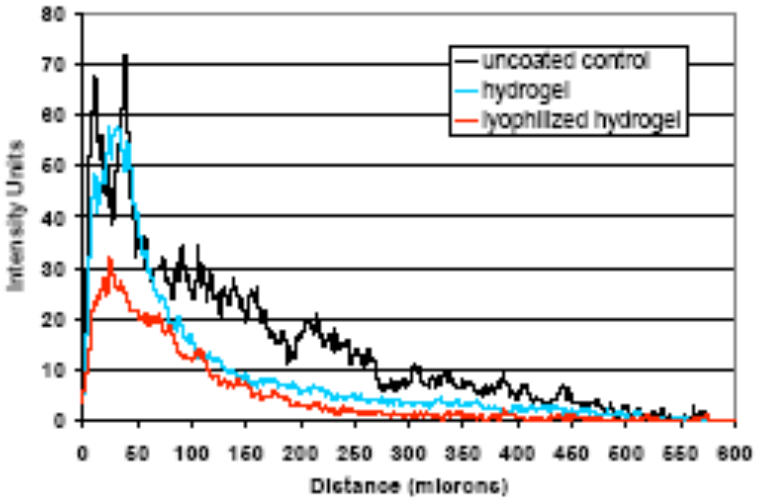

Figure U6-2. Average GFAP intensity as a function of distance from electrode interface.

References: Quarterly Report #6

Biran, R., Martin, D. C., & Tresco, P. A. (2005). Neuronal cell loss accompanies the brain tissue response to chronically implanted silicon microelectrode arrays. *Experimental Neurology*, *195*(1), 115-26.

Aim 4: Implanted probes show a stratified cellular response consisting of microglia, activated glial, and neural loss around the probe

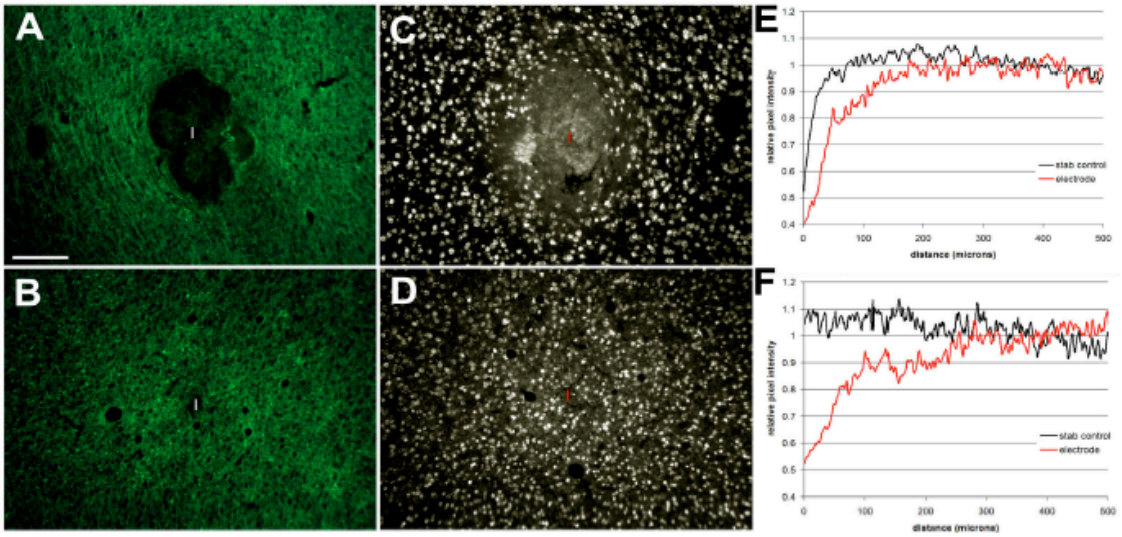

Figure U11-1. Reduction in neuronal fiber and bodies surrounding implanted silicon microelectrode arrays. Representative images at 2 weeks of neurofilament immunoreactivity (A,B) and NeuN immunoreactivity (C,D) in horizontal sections comparing implanted electrode (A,C) to a stab wound control (B,D) in the rat motor cortex. The implant cross section is marked by a vertical bar in each image. Scale bar = 200 microns. Quantitative analysis (N=at least 5 animals per group) of averaged neurofilament reactivity as a function of distance from the implant interface. All data from each image used for measurements were normalized to neurofilament intensity in the contralateral hemisphere. Hence, a relative intensity of 1 is normal. A student's t-test ($p<0.05$) of the area under the curve indicated significant differences between stab wound controls and implanted electrodes from 0 to 150 microns at 2 weeks (E) and from 0 to 200 microns at 4 weeks (F).

References: Quarterly Report #11

Biran, R., Martin, D. C., & Tresco, P. A. (2005). Neuronal cell loss accompanies the brain tissue response to chronically implanted silicon microelectrode arrays. *Experimental Neurology*, *195*(1), 115-26.

Aim 4: Tethering implanted microelectrodes to skull bone in the absence of electronic hardware elicits a similar tissue response to animals implanted with full electronic hardware headstage and cabling

Long-term tissue response studies in freely behaving rats with attached cabling are complicated by failures that result for animals removing headstages mounted with bone screws and acrylic cement. To compensate for the loss of animals and other such failure mechanisms large numbers of animals need to be enrolled in studies, which can be quite expensive. In addition, the motion resulting from grooming and other spontaneous animal behaviors may result in tissue responses at the electrode site that have nothing to do with the biomaterial coating or the composition of the electrode. To deal with these issues we developed a more economical animal model of brain reactivity which involves tethering the implanted electrode to the skull with silastic adhesive as shown in the figure above. Our analysis described in progress reports 8 and 9 showed that this approach results in a statistically similar tissue response with no loss of implanted animals.

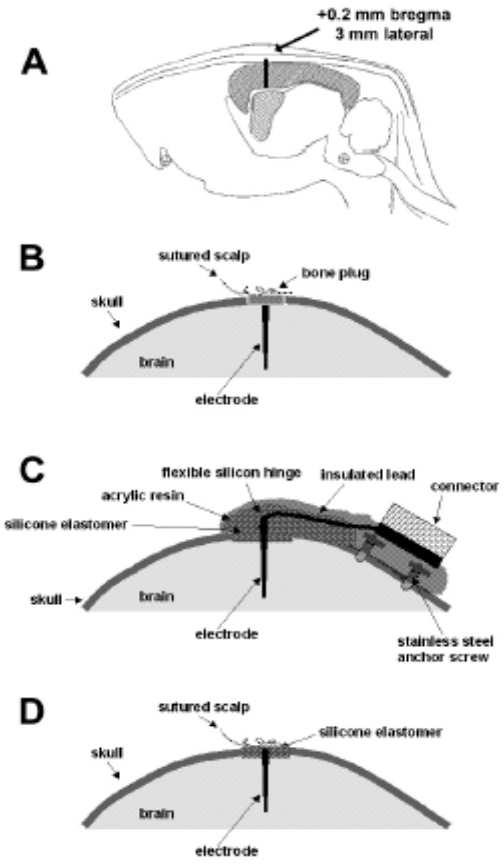

Figure 1. Schematic of implantation procedures. A) Location of microelectrode implant. B) Untethered microelectrodes. C) Conventionally tethered. D) Silastic tethered.

Reference:

Biran, R., Martin, D. C., & Tresco, P. A. (2005). Neuronal cell loss accompanies the brain tissue response to chronically implanted silicon microelectrode arrays. *Experimental Neurology*, *195*(1), 115-26.

Aim 4: Tethering increases cortical tissue reactivity to implanted silicon microelectrode arrays

The study examined the influence of electrode tethering on the adjacent brain tissue reaction over time by comparing different models of anchoring the same type of microelectrode. Our results indicated that the method of tethering significantly affects cortical brain tissue biocompatibility at the microelectrode interface and adjacent tissue, and that such changes influence the viability of nearby neurons.

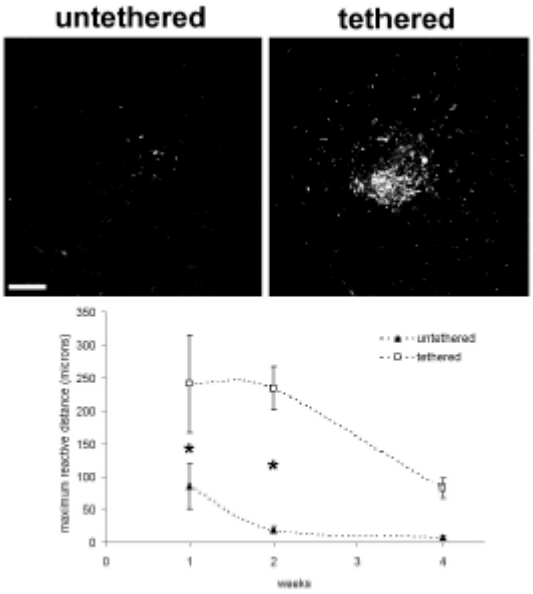

Figure 2. Comparison of ED1 reactivity. Representative photos of ED1 immunoreactivity surrounding microelectrode implants after 4 weeks duration. The graph plots mean maximal reactive distance of all specimens from 1 to 4 weeks. Scale bar = 100 microns. * Significant with $p<0.05$.

Reference: Biran, R., Martin, D. C., & Tresco, P. A. (2005). The Brain Tissue Response to Implanted Microelectrode Arrays is Increased When the Device is Tethered to the Skull. Journal of Biomedical Materials Research: Part A (under review).

Aim 4: Tissue response to implanted silicon microelectrode array is unchanged at 12 weeks post implantation and does not vary with rat strain

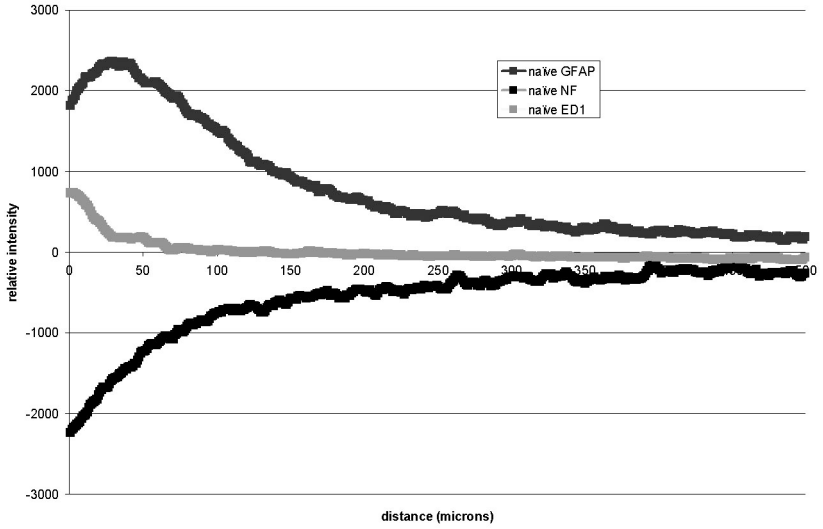

U15-3: Overall pattern of immunoreactivty for GFAP (uppermost line), ED-1 (gray line), and Neurofilament (lower line) for cortical tissue adjacent to microelectrodes implanted for 12 weeks.

Reference: Quarterly Report #15

Aim 4: Retrieved hydrogel coated microelectrode arrays contain hydrogel after 2, 4 and 12 weeks in rat cortex

Figure below shows that retrieved hydrogel-coated arrays still contain adherent tissue (a,b) and hydrogel coating (c,d). a,b) Corresponding brightfield and fluorescence images of the same retrieved HG-coated array demonstrate coverage with a highly ED-1 positive layer of macrophages / microglia. Arrow in (a) indicates translucent adherent tissue. c,d) Composite brightfield and DAPI-stained retrieved LHG-coated electrodes. Arrows indicate a nuclear translucent material, possibly remnants of the original coating. Scale bars = 200microns (a,b), 100 microns (c,d).

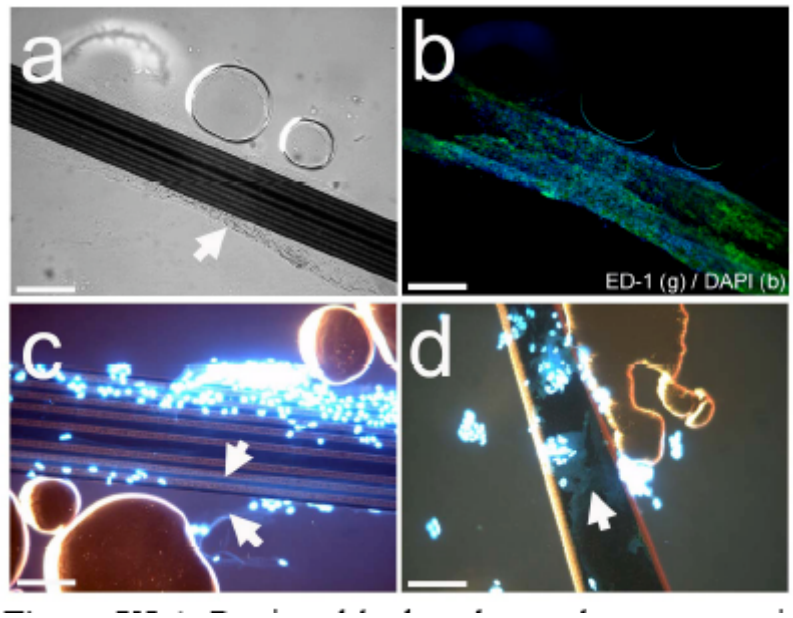

References: Quarterly Report #5

Aim 4: Loss of neuron associated neurofilament is abrogated by hydrogel coatings

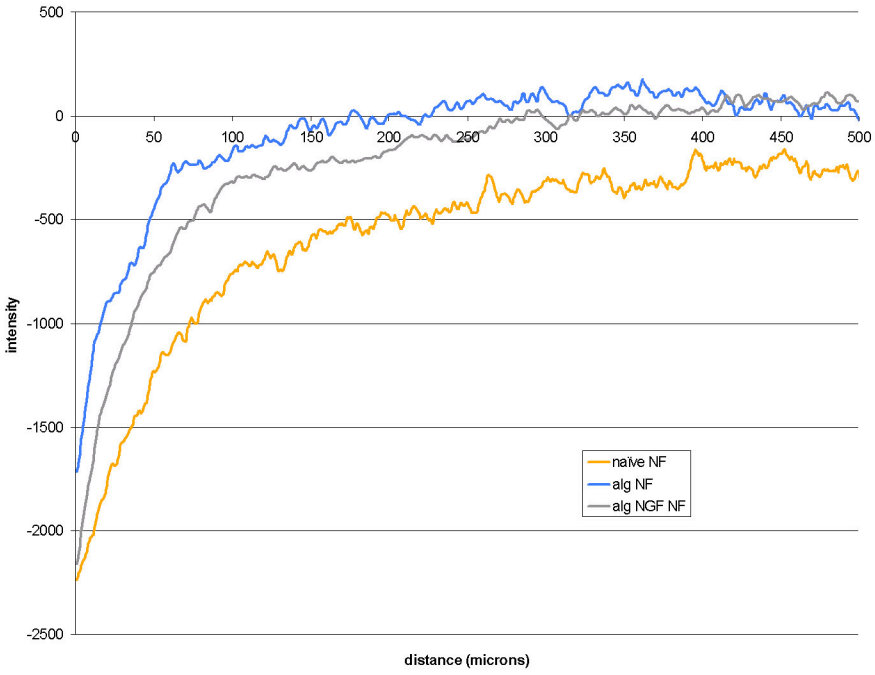

U15-6: Average cortical brain tissue immunoreactivity for neurofilament as a function of distance from the electrode into adjacent brain tissue 12 weeks after implantation of uncoated microelectrode arrays (Orange), Alginate coated microelectrode arrays (blue) and microelectrode arrays coated with alginate and loaded with NGF (gray). The general trend was that alginate treatment shifted the curves upward and to the left. The data is in agreement with our subjective interpretation of the histology reported in previous quarterly reports that alginate coated electrodes decrease the loss of neurons adjacent to indwelling microelectrodes over a three month period.

Reference: Quarterly Report #15

Aim 4: NGF incorporated into alginate coatings elicits a specific response in-vivo (ChAT)

The expression of choline actetyltransferase (ChAT) was examined in cells surrounding alginate and alginate-NGF microelectrodes. Immunostaining with ChAT antisera revealed an upregulation of the enzyme in cell bodies surrounding NGF-alginate microelectrodes (Figure U10-4). ChAT was also observed in a subset of neuronal fibers near the implant interface. Hence there appears to be an NGF-mediated effect on ChAT expression in the proximal neuropil, extending 8 to 10 cell layers away from the interface. While ChAT immunoreactivity in nearby fibers is most likely neuronal, the identity of the ChAT immunoreactive cell bodies has not yet been determined. This is currently being examined. In our progress to date regarding the alginate coating method, we have learned that the alginate coating stays intact during implantation and does not increase reactivity, that reactive inflammatory cells, mostly $ED1^+$ in identity, are still found on the surface of implanted microelectrodes. There is little to no evidence of neuronal damage in the zone surrounding the alginate-tissue interface. NGF can be trapped and released in detectable levels from alginate-coatings that have been dehydrated. Compared with control alginate coatings, NGF-containing alginate coatings do not appear to alter the normal pattern of inflammation and gliosis around implanted microelectrodes, and NGF-alginate coatings appear to influence the expression of ChAT in nearby cells.

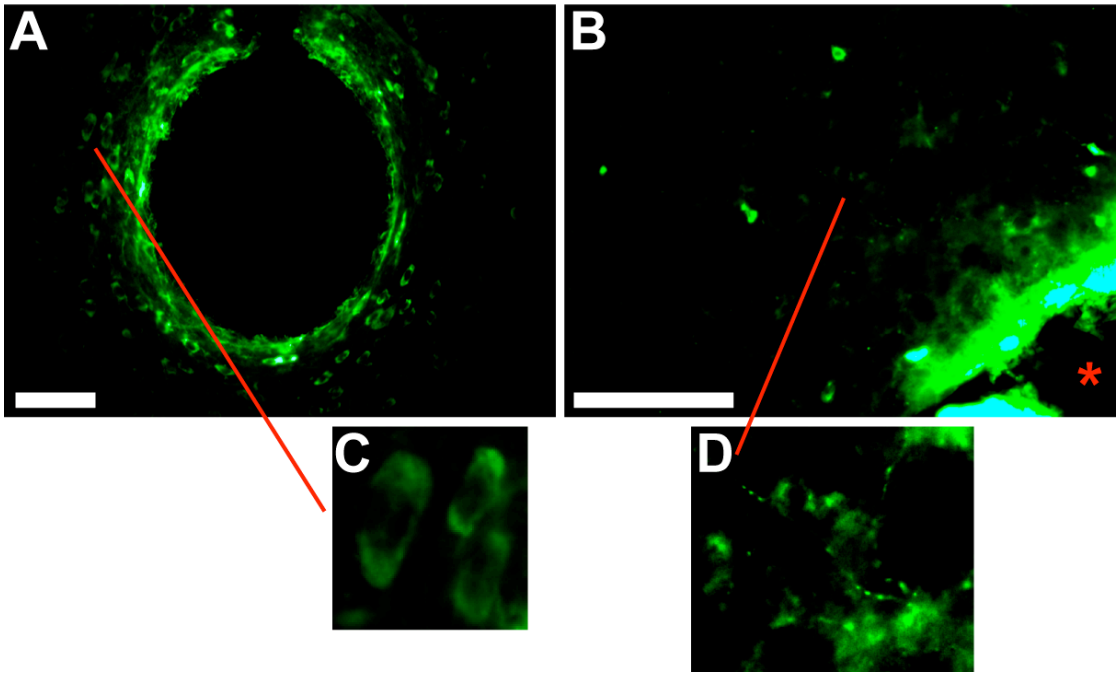

Figure U10-4. ChAT immunoreactivity is observed in cell bodies (A,C) and neuronal fibers (B,D) surrounding NGF-alginate coated microelectrodes. C,D are zoomed from portions of panels (A) and (B), respectively. Scale bars = 100 microns. Red asterisk in (B) marks the microelectrode track. Red arrows in (D) indicate a $ChAT^+$ fiber with a characteristic beaded pattern of reactivity.
Reference: Quarterly report #10.

Aim 4: Brain tissue reactivity is reduced adjacent to OEC-coated silicon microelectrode arrays

Primary syngeneic olfactory ensheathing (OEC) cells labeled with green fluorescent protein (GFP) were coated onto chronic single shank CNCT electrodes, cultured to 100% confluence (Figure U9-1), and implanted into the cerebral cortex for a period of 2 weeks using the silastic tethering procedure described in the previous report (see Progress Report #8). Images were taken from immunostained horizontal sections from all animals (cohort sizes of n=6 OEC coated, n=7 control uncoated). Compared with uncoated controls, the extent of both ED1 and GFAP reactivity was significantly reduced (Figure U9-1). The influence of the OEC coating to abrogate the extent of microglial reactivity (43% reduction) was relatively larger than the influence on GFAP reactivity, which was reduced by 22%. While the mechanism by which OEC exert this effect is not known, these data suggest that it is possible to use a cell-based coating to reduce glial reactivity surrounding a chronic CNS implant.

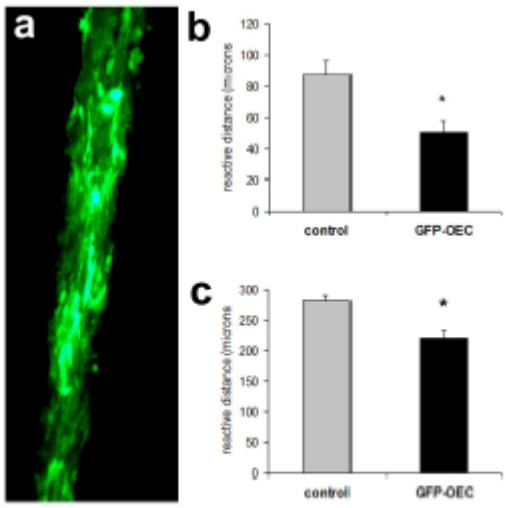

Figure U9-1. Reactivity is reduced around OEC-coated electrodes. a) Confluent EGFP-labeled cells on the shaft of a single shank CNCT electrode prior to implantation. Reduced maximal ED1 (b) and GFAP (c) reactive distance compared with uncoated controls at 2 weeks. * $p<0.05$ student's t-test.

Reference: Quarterly report #11

Aim 4: PEDOT coatings lead to improved recordings in-vivo

In collaboration with Prof. Daryl Kipke's group, we measured the performance of PEDOT-coated neural probes as a function of time in rat cortex. We found that the PEDOT-coated electrodes had lower impedance and systematically higher quality recordings. The recordings were stable for extended periods of time (6 weeks or more).

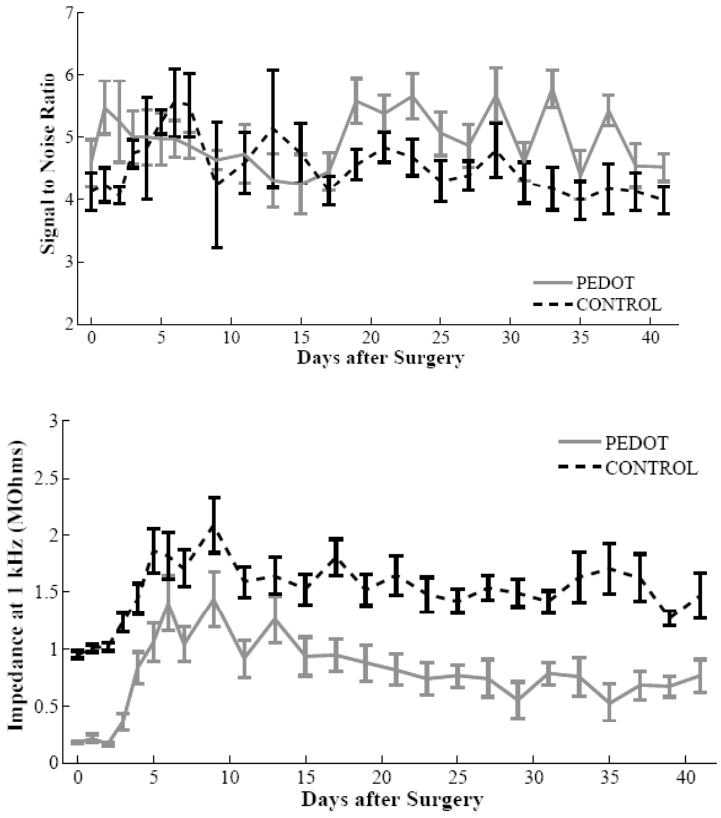

Top: 1 kHz impedance of implanted PEDOT-coated and uncoated probes as a function of time in rat cortex. Bottom: Recording quality (SNR ratio) as a function of time for PEDOT-coated and uncoated probes implanted in rat cortex.

Reference: Ludwig, K., Yang, J., Martin, D. C., & Kipke, D. R. (2005). In-Vivo Performance of PEDOT-Modified Neural Probes. *Journal of Neural Engineering*, *in press.*

Aim 5: PEDOT can be coated on Utah multishank electrodes

We obtained Utah electrodes from Richard Normann (Utah) and Richard Stein (Alberta). We demonstrated that the PEDOT decreased the impedance, but not as dramatic as in Michigan probes (~3X decrease in impedance, as opposed to ~100X decrease seen on other probe designs). We still need to further optimize coating procedures since area of conducting surface on the doped-silicon electrode tips are not well characterized in this design.

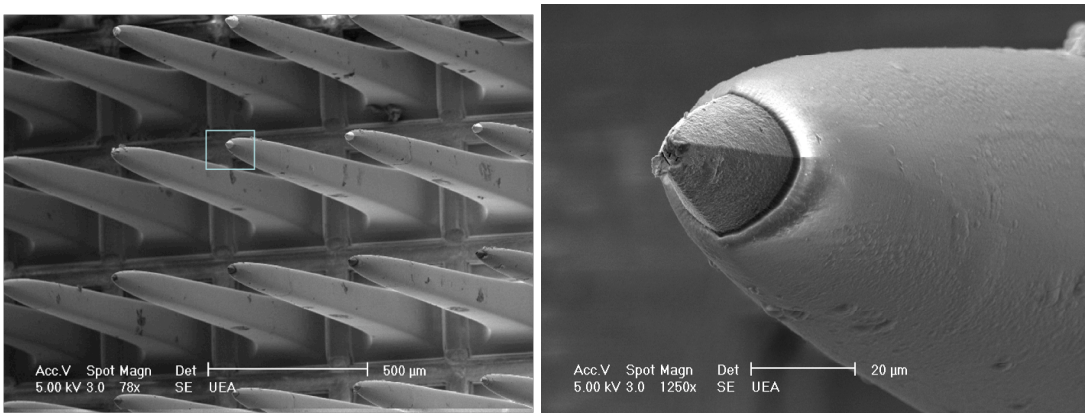

Left: SEM image of PEDOT-coated multishank Utah-style electrode array. Right: Close-up view of the PEDOT-coated electrode tip.

Aim 5: PEDOT can be coated onto ball electrodes

We received some Pt-Ir ball electrodes from Prof. Yoash Raphael in Otolaryngology and coated these with PEDOT as well. These ball electrodes are used in cochlear implants. We saw a dramatic decrease in impedance (~100X), as we have now seen on many other electrode geometries.

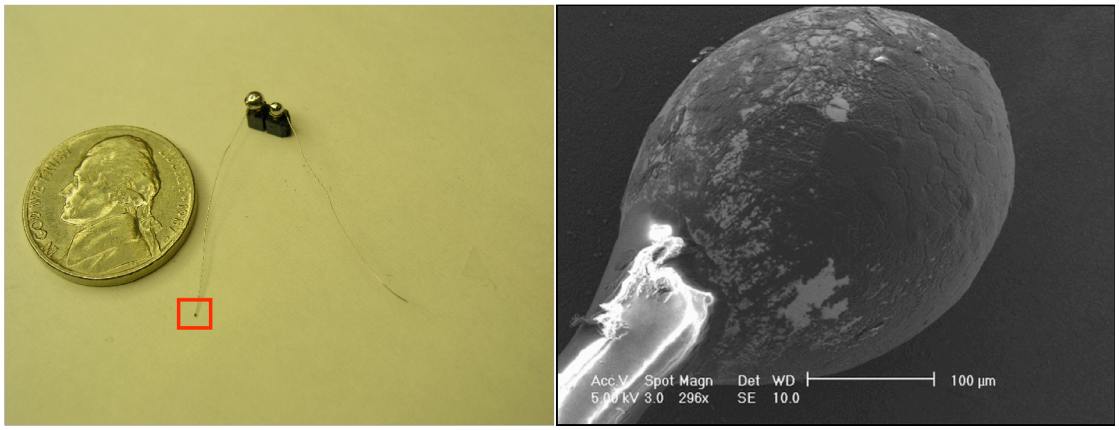

Left: optical micrograph of ball electrode. Right: SEM image of PEDOT-coated ball electrode.

Aim 5: PEDOT coated onto a wide variety of other electrodes (Stanford, Applied Biophysics, custom-designed geometries).

We have coated PEDOT onto electrodes from Gregory Kovacs at Stanford (below), commercial electrodes from Applied Biophysics (www.biophysics.com), and custom-designed geometries developed in our own laboratory

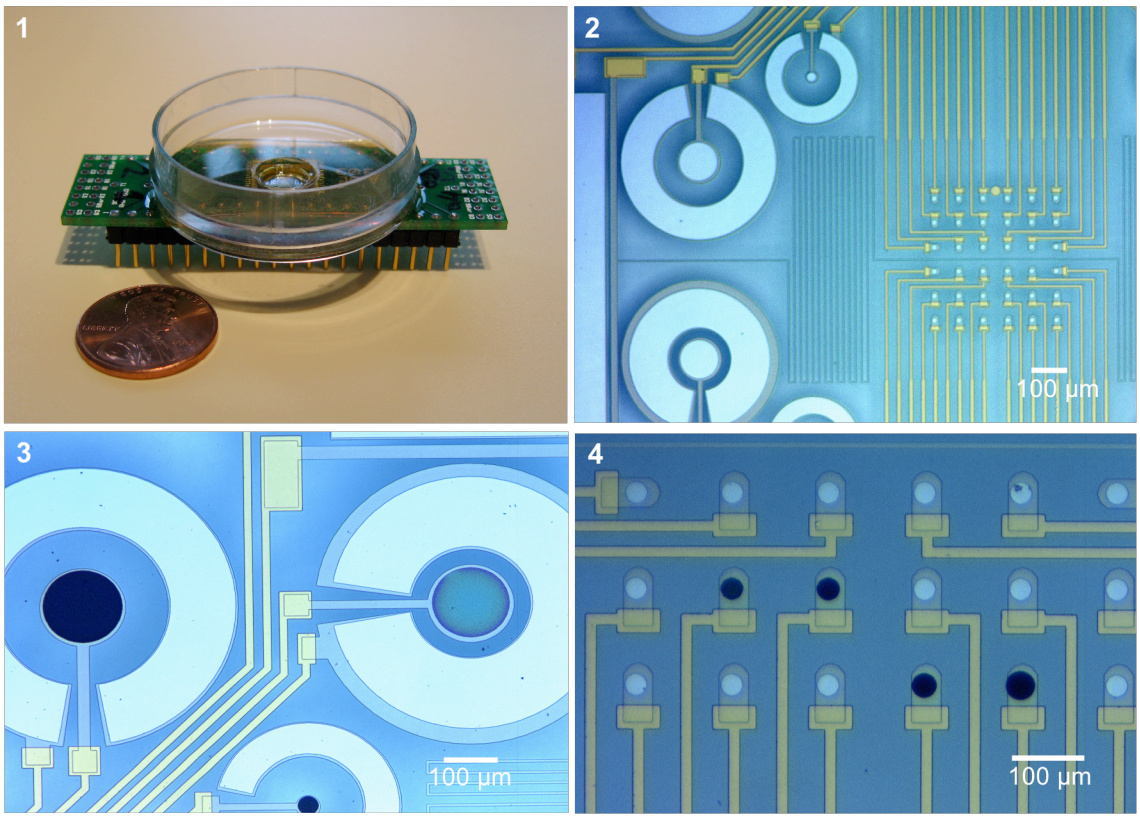

1. Culture dish electrode array fabricated by Kovacs Group, Stanford University.
2. Silicon microelectrode array with unmodified metallic stimulating, recording, and heating electrodes.
3. PEDOT-PSS coated onto platinum stimulating electrodes by Martin Group, University of Michigan.
4. Various thicknesses of PEDOT-PSS deposited onto the recording array.

Aim 5: PEDOT coated onto cochlear implants, pacemakers

We have coated PEDOT onto multi-electrode cochlear implants, and cardiac pacemakers. Shown below is a PEDOT-coated pacemaker electrode from Guidant, provided to us by Dr. Frank Pelosi from Cardiology at the University of Michigan. PEDOT was successfully coated onto the spiral recording electrode as well as the cuff stimulating electrode.

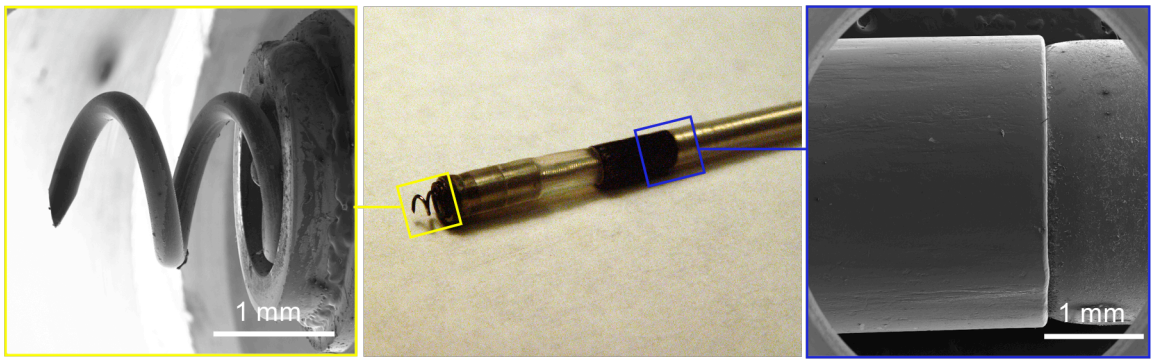

Left: SEM spiral recording electrode coated with PEDOT. Middle: macroscopic view of Guidant pacemaker electrode coated with PEDOT. Right: cuff stimulating electrode coated with PEDOT.

What was not achieved\

One of our goals was to develop nanofibrous films to maximize the amount of surface area to decrease impedance and improve the mechanics of the polymer films. Block copolymer templated films made "nanomushrooms", not the long hairs as was originally desired. This goal was eventually achieved using anionic polymeric counterions such as poly(acrylic acid). The nanomushroom shapes may have interest for other applications. References: Quarterly Report #3

We tried polymerizations inside cubic phases of surfactants to give bicontinuous ordered structures. Although we were not able to find a system with a cubic phase region of stability wide enough to remain ordered during the reaction, we have recently found a monoglyceride system that has an extended range of stability in both composition and temperature (.

We did only limited investigations of the L1 adhesion protein. The L1 protein proved to be more difficult and expensive to obtain, and our investigations of more readily available (and more well known) neurotrophin NGF proved to give us the feasibility information needed to optimize processing and bioactivity characterization.

We determined that in-vivo results were a more accurate measure of the required response, and therefore focused our efforts here rather than on in-vitro experiments. We have not yet gathered much feedback on the electrical properties of probes implanted in-vivo. We did do a comprehensive study on PEDOT-modified probes with Kipke, although more work is done to confirm these results and examine the influence of different material designs. We also need to correlate in-vivo electrical properties measurements with histology around the implanted probe. We examined the influence of dexamethasone-loaded hydrogel modified probes with Anderson, but we still need to compare these results with more controls to elucidate the influence of specific contributions to these observations (such as unmodified hydrogels without dexamethasone).

Recommendations for future research and development

Based on the results of our research, we have several recommendations for future research and development. These include:

(1) Can nanofibrous conducting polymer networks be created that can extend across the glial scar?

We have established techniques for creating nanofibrous networks of conducting polymers that can be grown directly on the electrode site. Is it possible to create films that allow for these filaments to extend across the glial scar, into the surrounding tissue? If so, probes modified with these materials ought to show much improved, stable long-term recordings.

(2) Can in-situ grown conducting polymer electrodes provide for improved performance?

The most revolutionary approach for modifying the electrode surface is to grow the conducting polymer in place directly in the tissue. How does this impact the viability of various cell types around the probe? Does this improve probe performance?

(3) How do polymer-modified electrodes perform in-vivo?

Our results to date show that PEDOT-modified electodes show lower impedance and improved quality of recordings. What are the optimal coating parameters required to improved this performance? This requires additional animal studies, and examinations of the histology around polymer-modified implanted probes.

(4) How do these materials perform in other applications?

We are particularly interested in using these concepts to improve the performance of other devices, such as cochlear implants. Here, the cochlear chamber may act as a reaction vessel, allowing us to establish stable, intimate connections with the spiral ganglion cells.

(5) Can melanins mimic or replace the role of PEDOT?

Natural pigments such as melanin have a conjugated backbone structure similar to that found in PEDOT. Melanin is the well-known, common pigment found in hair and skin. It is also found in the Substantia Nigra, but its biological role here is unclear. It is known that melanin can be deposited electrochemically, and it may provide an alternative to PEDOT that is more biocompatible. It will be necessary to determine the optimal means for depositing melanins, and compare this with established results on PEDOT.